Title

Effects of experimental nitrogen deposition on soil organic carbon storage in Southern California drylands

Journal

Global Change Biology, 29(6)

ISSN

1354-1013

Authors

Püspök, Johann F
Zhao, Sharon
Calma, Anthony D
et al.

Publication Date

2023-03-01

DOI

10.1111/gcb.16563

Peer reviewed

Title:

Effects of experimental nitrogen deposition on ~~dryland~~ soil organic carbon storage in southern California drylands

Authors:

Johann F. Püspök[1*] (ORCID: 0000-0001-6946-1030), Sharon Zhao[1], Anthony D. Calma[1], George L. Vourlitis[2] (ORCID: 0000-0003-4304-3951), Steven D. Allison[3,3a] (ORCID: 0000-0003-4629-7842), Emma L. Aronson[4] (ORCID: 0000-0002-5018-2688), Joshua P. Schimel[5] (ORCID: 0000-0002-1022-6623), Erin J. Hanan[6] (ORCID: 0000-0001-6568-2936), Peter M. Homyak[1] (ORCID: 0000-0003-0671-8358)

1. Department of Environmental Sciences, University of California, Riverside CA 92521, USA

2. Department of Biological Sciences, California State University, San Marcos, CA 92096, USA.

3. Department of Ecology and Evolutionary Biology, University of California, Irvine CA

3a. Department of Earth System Science, University of California, Irvine CA

4. Department of Microbiology and Plant Pathology, University of California, Riverside CA 92521, USA

5. Department of Ecology, Evolution, and Marine Biology and Earth Research Institute, University of California, Santa Barbara, CA 93106, USA

6. Department of Natural Resources and Environmental Science, University of Nevada, Reno

***Corresponding author:**

Johann F. Püspök, Department of Environmental Systems Science, ETH Zurich, Universitätsstrasse 16, 8092 Zurich, Switzerland. Email: johann.puespoek@email.ucr.edu. Phone: +43 664 1432 732.

Key points

Type any here or delete

Keywords

Soil carbon storage, atmospheric nitrogen deposition, ~~drylands,~~ particulate organic matter (POM), mineral-associated organic matter (MAOM), carbon use efficiency, soil acidification, fertilization, soil microbes, extracellular enzymes ~~activities~~

Abstract

Atmospheric nitrogen (N) deposition is enriching soils with N across biomes. Soil N enrichment can increase plant productivity and microbial activity, thereby increasing soil organic carbon (SOC), but such responses vary across biomes. Drylands cover ~45% of Earth's ~~the~~ land area and store ~32~~3~~% of ~~the~~ global SOC contained in the top 1m of soil ~~global carbon stocks.~~, ~~meaning~~ Nitrogen fertilization could, ~~can~~ therefore, disproportionately impact carbon (C) cycling, yet whether dryland SOC storage increases with N remains unclear. To understand how N enrichment may change SOC storage, we separated SOC into plant-derived, particulate organic ~~carbon~~ C (POC), and largely microbially-derived, mineral-associated organic ~~carbon~~ C (MAOC) at four N deposition experimental sites in Southern California. Theory suggests that N enrichment increases the efficiency by which microbes build MAOC (~~carbon~~ C stabilization efficiency) if soil pH stays constant. But if soils acidify, a common response to N enrichment, then microbial biomass and enzymatic organic matter decay may decrease, increasing POC but not MAOC. We

found that N enrichment had no effect on soil ~~carbon~~ C fractions except for a decrease in MAOC at one site. Specifically, despite reported increases in plant biomass in three sites and decreases in both microbial biomass and extracellular enzyme activities in two sites that acidified, POC did not increase. Furthermore, microbial ~~carbon~~ C use and stabilization efficiency increased ~~in long-term incubations~~ in a non-acidified site, but without increasing MAOC. Instead, MAOC decreased by 16% at one of the sites that acidified, likely because it lost 47% of the exchangeable calcium (Ca) relative to controls. Indeed, MAOC was strongly and positively affected by Ca, which directly and, through its positive effect on microbial biomass, explained 58% of the variation in MAOC. Long-term effects of N fertilization on dryland SOC storage appear abiotic in nature, such that drylands where Ca-stabilization of SOC is prevalent and soils acidify, are most at risk for significant ~~carbon~~ C loss.

Introduction

Atmospheric nitrogen (N) deposition has tripled since 1850 due to emissions from agriculture and fossil fuel burning, leading to a global enrichment of soil N pools (Gruber and Galloway 2008; Kanakidou et al. 2016). This N enrichment affects plant growth and microbial activity and, thereby, strongly interacts with the global carbon (C) cycle (Gruber and Galloway 2008; Treseder 2008; O'Sullivan et al. 2019). Soil organic C~~carbon~~ (SOC) contains more C than vegetation and the atmosphere combined and confers important soil functions such as soil fertility and water retention (Weil and Brady 2017). Globally, SOC pools have increased by 4.2% in response to N enrichment (Xu et al. 2021), but responses can be biome-specific (Deng et al. 2020). Drylands make up ~45% of the global land area and store up to 33~~2~~% of the global SOC stocks contained in the top 1m of soil (Prăvălie 2016; Plaza et al. 2018b). Therefore, dryland response to N deposition could have substantial consequences on global C cycling and soil quality (Homyak et al. 2014; Plaza et al. 2018a;

Osborne et al. 2022), but they are underrepresented in global analyses evaluating N fertilization effects on soil C storage (Xu et al. 2021). While both increases and decreases in SOC have been measured along N deposition gradients in drylands (Ochoa-hueso et al. 2013; Maestre et al. 2016), the magnitude of and mechanisms behind dryland C storage change in response to N deposition remain unclear.

The effects of N enrichment on SOC storage depend on many factors including changes in plant C inputs, organic matter decomposition, microbial transformations of C compounds, and stabilization of C through interactions with soil minerals (Janssens et al. 2010; Castellano et al. 2015; Ye et al. 2018). To help identify changes in SOC storage and the mechanisms governing the fate of C in response to N deposition, SOC can be separated into two pools of different origin and persistence (Lavallee et al. 2020): i) a relatively fast cycling, particulate organic C (POC) fraction, consisting of relatively undecomposed plant material, and ii) a relatively slow cycling, mineral-associated organic C (MAOC) fraction, consisting of heavily decomposed plant compounds and microbial products (Lavallee et al. 2020; Whalen et al. 2022). Due to their differences in formation, variation in the largely plant-derived POC fraction is thought to depend mostly on N-induced changes in decomposition and plant biomass production (Rossi et al. 2020), with roots considered important in drylands where much of aboveground biomass can decompose before being incorporated into the soil (Berenstecher et al. 2021). In contrast, variation in MAOC is thought to depend more on changes in litter quality, microbial metabolism, and soil sorption potential (Fig. 1) (Castellano et al. 2015; Sokol et al. 2019). Previous research separating SOC into POC and MAOC has shown that N fertilization effects on C storage in semi-arid grasslands were mostly driven by increased aboveground biomass and POC, but microbial C cycling and

92 mineral stabilization in the MAOC pool may be also important (Ye et al. 2018; Lin et al.
93 2019).

94 Microbial C cycling can affect MAOC pools through the in-vivo transformation of C
95 compounds—also known as the "microbial C pump"—into microbial biomass and microbial
96 by-products (Liang et al. 2017). Carbon that cycles through the "pump" via microbial death
97 or exudation can then associate with mineral surfaces and become protected from further
98 microbial decomposition (Islam et al. 2022). Therefore, microbial C use efficiency (CUE),
99 the fraction of C uptake that is allocated to biomass growth, is key to determining SOC
100 storage (Bradford et al. 2013). Microbial CUE is often measured by tracing microbial uptake
101 and respiration of isotopically-labelled C compounds, which depends on many factors
102 including microbial community composition, climate, soil physicochemical conditions, and
103 soil nutrient status (Manzoni et al. 2012a; Jones et al. 2019; Butcher et al. 2020; Pold et al.
104 2020). Microbial C~~carbon~~ stabilization efficiency (CSE) extends the CUE term by accounting
105 for the formation of microbial residues that can be stabilized in soil, and can thus link N-
106 induced changes in microbial physiology with long-term C stabilization, particularly when
107 measured over longer time periods (e.g., multiple weeks) (Geyer et al. 2020). Studies in
108 temperate grasslands found that adding N increased CUE and SOC storage (Poeplau et al.
109 2019). However, in drylands, microbes may be limited by C or there may be no link between
110 CUE and MAOC formation because dryland soils are typically coarse-textured with low C
111 sorption potential (Schaeffer et al. 2003; Creamer et al. 2014, 2016; Cai et al. 2022). How
112 microbial CSE or CUE change in response to N enrichment has not been measured before in
113 drylands, and it is not known whether atmospheric N deposition can affect SOC storage via
114 changes to the microbial C pump.

The effects of atmospheric N deposition on SOC storage may also depend on whether N enrichment acidifies soils. For example, ecosystem models suggest N enrichment should favor the transformation of POC into persistent MAOC, but only if decomposition is N-limited and soils do not become too acidic to adversely affect microbial physiology (Averill and Waring 2018). However, acidification is a common response to N enrichment resulting from H^+ release during nitrification, H^+ release after plants take up NH_4^+, and leaching of base cations as companion ions to NO_3^- (Tian and Niu 2015). Thus, many studies attribute increases in SOC after N enrichment to acidity-induced decreases in microbial biomass and decreased organic matter decomposition, which lead to a build-up of POC without further breakdown to MAOC (Treseder 2008; Janssens et al. 2010; Riggs and Hobbie 2016; O'Sullivan et al. 2019). Notably, even more alkaline drylands, considered to be well-buffered against changes in pH (Slessarev et al. 2016), can acidify even in non-experimental settings (Yang et al. 2012). Identifying which mechanism governs SOC dynamics has, therefore, been challenging. ~~, especially because drylands can be well-buffered against changes in pH (Slessarev et al. 2016), presumably protecting microbes from acidification and maintaining decomposition.~~ One way to overcome this challenge is to measure changes in the activity of extracellular enzymes. Because decomposition and changes in SOC are largely driven by enzymes that break down polymers into smaller, more easily assimilated compounds (Burns et al. 2013), extracellular enzyme activities may offer an opportunity to disentangle whether acidification affects microbial decomposition (e.g., a decrease in decomposition may correlate with reduced enzyme activity), the partitioning of SOC, and the fate of both POC and MAOC pools.

Beyond the direct effects of acidification on microbial physiology, and cascading effects on POC and MAOC pools, MAOC may change directly in response to changes in soil

physicochemical conditions. For example, whether MAOC persists in soil largely depends on the number of sorption sites available for binding C (Castellano et al. 2015; Cotrufo et al. 2019). In dryland soils, SOC stabilization is thought to be primarily controlled by clay content and exchangeable calcium (Ca) (Rasmussen et al. 2018), as polyvalent cations, like Ca, can stabilize SOC by bridging negatively charged C compounds with negatively charged mineral surfaces or by binding together multiple organic molecules (Rowley et al. 2018). In fact, N enrichment can destabilize Ca-bridges and MAOC via Ca leaching from acidification (Ye et al. 2018; Wan et al. 2021), but it is unclear how widespread such pH-induced MAOC losses are in relatively well-buffered dryland soils.

Long-term N fertilization experiments are powerful tools for understanding how N fertilization and changes in soil physicochemical properties may influence SOC dynamics, because they add known amounts of N while reducing natural variation in confounding factors (e.g., plant species, soil taxonomy, climate, etc.) often present in studies along natural N deposition gradients. In this study, we use four sites in long-running (i.e., > 134 years) N fertilization experiments across drylands in Southern California: one grassland site, two sites in deciduous shrub-dominated coastal sage scrub (CSS), and one site in evergreen shrub-dominated chaparral. Three of the four studied sites increased in AGB in response to N fertilization (Parolari et al. 2012; Vourlitis et al. 2021a). To study how N enrichment and acidification may differently affect SOC fractions, two of the sites were fertilized with urea, NH_4^+, and NO_3^-, and showed calcium leaching and strong acidification, whereas the two other sites were fertilized with $CaNO_3$ to prevent acidification. Specifically, we ask: How does long-term N fertilization affect C storage in POC and MAOC fractions under acidifying versus non-acidifying conditions? And does N fertilization change the stabilization efficiency of labile C inputs via the microbial C pump?

We answered these questions using a combination of size and density fractionations to separate soils into POC and MAOC pools. To explore which mechanisms may control changes in soil C fractions, we measured changes in exchangeable Ca as an index for how C stabilization potential was affected by N fertilization, and microbial biomass and enzyme activities as an index for how microbial decomposition was affected by N fertilization. Furthermore, we assessed ~~carbon~~ C stabilization efficiency (CSE) and ~~carbon~~ C use efficiency (CUE) by measuring the efficiency by which microbes retained ^{13}C-labelled glucose in soil, during both short- and long-term incubations. We hypothesized that a) the previously reported increase in plant growth in response to N addition at three of the sites (Parolari et al. 2012; Vourlitis et al. 2021a) would increase POC, particularly in acidified plots where decomposition might be inhibited; b) N enrichment would increase CSE and the transformation of POC into MAOC in non-acidified plots; and c) N enrichment would decrease exchangeable Ca and MAOC in acidified plots.

Material and Methods

Sites description

Our study was conducted at three long-running N fertilization experiments in Southern California that together consist of four sites and represent the three dominant vegetation types in the region: ~~(~~chaparral, coastal sage scrub (CSS), and grassland~~)~~. The chaparral site (CHAP) is located at the Sky Oaks Field Station in San Diego County, CA (33.381 N, 116.626 W, elev. 1420 m). The first CSS site (CSS1) is located at the Santa Margarita Ecological Reserve in Riverside County, CA (33.438 N, 117.181 W, elev. 248 m). The grassland site (GRASS) and second CSS site (CSS2) are part of the Loma Ridge Global Change Experiment located at Irvine Ranch National Landmark in Orange County, California (33.742 N, 117.704 W, elev. 365 m). All sites have a Mediterranean climate with cool, wet

winters and hot, dry summers; most rain falls between November and April. Important site information is summarized in Table 1 and described in more detail below.

CHAP and CSS1 are extensively described in Vourlitis et al. (2021). Mean annual precipitation at CHAP is 382 mm. Vegetation is dominated by *Adenostoma fasciculatum* and *Ceanothus greggii*. Soils are Entic Ultic Haploxerolls (Sheephead series) derived from micaceous shist and have a loamy sand texture (Supp. Table 2). The site burned at the onset of the N fertilization experiment in 2003. CHAP experienced severe acidification in response to N fertilization, with soil pH decreasing by 1.65 pH units below control plots in 2021 (Table 2). Mean annual precipitation at CSS1 is 414 mm. Vegetation is dominated by *Artemisia californica* and *Salvia mellifera*. Soils are Typic Rhodoxeralfs formed from weathered Gabbro material (Las Posas series) and have a sandy loam texture (Supp. Table 2). CSS1 experienced severe acidification in response to N fertilization, with soil pH decreasing by 1.49 pH units below control plots in 2021 (Table 2). CHAP and CSS1 have the same experimental layout, consisting of 8 plots in 4 pairs. Each pair consists of one 10 × 10 m control plot and one 10 × 10 m N-fertilized plot. Plots have been fertilized with 50 kg N ha^{-1} y^{-1} every fall since 2003 as either NH_4NO_3 (2003–2007), $(NH_4)_2SO_4$ (2007–2009), or urea (2009–present). Background N deposition rate at both sites is estimated as 2-4 kg N ha^{-1} y^{-1} (Fenn et al. 2010).

Vegetation at the Loma Ridge Global Change Experiment consists of a mosaic of non-native annual grassland and CSS and hosts the GRASS and CSS2 sites. Mean annual precipitation is 281 mm (Khalili et al., 2016). Vegetation at GRASS mostly includes *Bromus diandrus*, *Lolium multiflorum* and *Avena fatua*. Abundant species at CSS2 include *Malosma laurina*, *Artemisia californica* and *Salvia mellifera* (Potts et al., 2012). Soils are Typic Palexeralfs (Myford series) formed on colluvial deposits from sedimentary rocks and have a

sandy loam texture (Khalili et al. 2016). GRASS and CSS2 have the same randomized split-plot design, consisting of 4 replicate plots that are split: half unfertilized and half fertilized with 60 kg N ha^{-1} y^{-1}. Plots have been fertilized since 2007 with 20 kg N ha^{-1} y^{-1} as immediate-release $CaNO_3$ prior to the wet season and 40 kg N ha^{-1} y^{-1} as 100-day release $CaNO_3$ during the wet season. Background atmospheric N deposition is estimated as 15 kg N ha^{-1} y^{-1} (Fenn et al. 2010). Fires burned the plots when fertilization started in 2007 and again in October 2020. The 2020 fire had no effect on soil bacterial community composition, microbial biomass or soil pH (Barbour et al. 2022; this study).

Soil sampling

Soils at all sites were sampled at the end of the dry season in October 2020, when most plants are senesced, and at the end of the wet season in April 2021, when most plants are actively growing. After removing plant litter from the soil surface, two soil sub-samples were taken from each plot using a soil auger (2.54 cm diameter × 10 cm depth) and combined into one composite sample. Soil samples were taken from randomly selected locations ~~in the grassland plots~~in the plots at GRASS and from underneath randomly selected shrubs in the plots at~~in the chaparral~~ CHAP, CSS1 and CSS2~~ plots~~. At CHAP~~Sky Oaks~~ and CSS1~~Santa Margarita~~, additional soil samples were taken from~~ the~~ locations with bare soil in the interspaces between shrub canopies~~s~~, yielding one “Beneath shrub” and one “Interspace” sample per plot. No interspace samples were taken at GRASS and CSS2~~Loma Ridge~~ since there was no significant area of bare soil without plant cover. We took samples from beneath shrubs and interspaces where possible because we expected biological processes more important in driving the response to N fertilization beneath shrubs and abiotic processes more important in interspaces. Soil samples were brought to the lab and sieved (2 mm) for all further analyses. Field-moist soil samples were kept at 4°C. All measurements on field-moist

soil samples were done within one week of sampling to minimize storage effects. Gravimetric water content was measured by drying field-moist soil samples at 104°C for 24h. All data are expressed on a per g dry weight basis.

Total C and N, soil pH, exchangeable Ca^{2+}, exchangeable NO_3^- and NH_4^+ and water-extractable organic C

The total soil C and N content was measured after combustion using a Flash EA 1112 NC analyzer (Thermo Fisher Scientific Inc., Waltham, MA). Soil pH was measured with a glass electrode on air-dried soil in nanopure water (1:2 (w:v) soil dry weight:solution). Exchangeable Ca^{2+} was measured in 0.1 M $BaCl_2$ extracts of air-dried soil (1:20 soil dry weight:solution) by inductively-coupled plasma optical-emission spectrometry (ICP–OES) using an Optima 7300 DV (Perkin-Elmer Inc., Shelton, CT) (Hendershot and Duquette 1986). Exchangeable nitrate (NO_3^-) and ammonium (NH_4^+) were measured in 2 M KCl extracts of field-moist soil (1:10 (w:v) soil dry weight:solution) on an AQ2 Discrete Analyzer (SEAL Analytical, Mequon, WI). Values below the limit of detection of the instrument were replaced with 0.003 mgN/L for NO_3^- and 0.05 mgN/L for NH_4^+. Water-extractable organic C (WEOC) was measured in nanopure water extracts of field-moist soil (1:10 (w:v) soil dry weight:solution) on a TOC-V_{CHS} analyzer (Shimadzu, Kyoto, Japan). All analyses were conducted at the Environmental Sciences Research Laboratory (ESRL) at UC Riverside (https://envisci.ucr.edu/research/environmental-sciences-research-laboratory-esrl).

Microbial biomass C and N

Microbial biomass C and N were measured with a chloroform slurry extraction (Fierer 2003). Subsamples of 10 g field-moist soil were shaken in 40 mL 0.5 M K_2SO_4 with or without addition of 0.5 mL chloroform. Chloroform was purged from the extracts by bubbling with room air for 30 minutes. Extracts were filtered (0.9 µm pore size) and analyzed

for organic C and N on a TOC-V_{CHS} analyzer coupled with a TNM-1 Total nitrogen measuring unit (Shimadzu, Kyoto, Japan) in the ESRL. Microbial biomass C and N were calculated as the difference in organic C or N between subsamples extracted with and without chloroform (Brookes et al., 1985; Vance et al., 1987). No correction factor for extraction efficiency was used and thus we report a "flush" in microbial biomass C after extraction.

Soil hydrolytic extracellular enzyme activities

Potential extracellular soil enzyme activities (see Table 3 for their function) were measured with fluorigenic substrates (Marx et al., 2001) as described in the Supporting Information and paired accordingly: (i) α-glucosidase (AG) with 4-methylumbelliferyl-α-D-glucopyranoside; (ii) 1,4-β-cellobiohydrolase (CBH) with 4-MUF-β-D-cellobioside (iii); ß-glucosidase (BG) with 4-methylumbelliferyl ß-D-glucopyranoside; (iv) N-acetyl-ß-D-glucosaminidase (NAG) with 4-methylumbelliferyl N-acetyl-ß-D-glucosaminide; (v) phosphomonoesterase with 4-methylumbelliferyl phosphate; and (vi) L-Leucine aminopeptidase (LAP) with L-Leucine-7-amido-4-methylcoumarin.

Soil organic matter fractionation

Soil organic matter was fractionated into POC, sand-associated organic C, and silt and clay-associated organic C using a combination of density and size fractionation modified from Soong & Cotrufo (2015). We separated MAOC into a sand fraction and a silt–clay fraction because they vary in turnover time, and the silt–clay fraction is considered more important in determining C stabilization (Poeplau et al. 2018). Therefore, from now on we will only consider the silt–clay fraction as MAOC. Size and density cutoffs were chosen based on conceptual work outlined in (Lavallee et al. (2020). Briefly, 5g of oven-dried soil was dispersed in 1.65 g cm^{-3} sodium poly-tungstate (SPT) by applying 200 J mL^{-1} ultrasonic energy at 60 W. After centrifugation (2500 g for 60 min), the floating light fraction

(representing POC) was aspirated and collected on a 0.45 µm glass fiber filter using a vacuum-filtration unit and rinsed with nanopure water. The heavy fraction pellet was washed with nanopure water and passed through a 53 µm sieve to separate the sand fraction (>53 µm) from the silt and clay fraction (<53 µm). All fractions were oven-dried (60°C), weighed and then finely ground. The ground fractions were analyzed for % C and % N on a Flash EA 1112 NC analyzer (Thermo Fisher Scientific Inc., Waltham, MA). During sample processing we recovered 100% ± 1% (mean ± standard deviation) of the soil mass, 108% ± 14% of the C and 106% ± 17% of the N.

Carbon stabilization efficiency and ~~carbon~~ C use efficiency

We estimated ~~carbon~~ C stabilization efficiency (CSE) and ~~carbon~~ C use efficiency (CUE) in the same incubation using the methods described by Geyer et al. (2020) and the following equations:

$$CSE = \frac{^{13}Soil\,C}{^{13}Soil\,C + ^{13}CO_2} \quad (1)$$

$$^{13}Soil\,C = Soil\,C \times \frac{at\,\%\,C_L - at\,\%\,C_{ref}}{at\,\%\,label - at\,\%\,C_{ref}} \quad (2)$$

$$^{13}CO_2 = cumulative\ ^{12}CO_2 \times \frac{at\,\%\,C_L - at\,\%\,C_{ref}}{at\,\%\,label - at\,\%\,C_{ref}} \quad (3)$$

Where *Soil C* = the total C in soil samples (µg C g^{-1} dry soil), *at% C_L* = the ^{13}C at% of labelled soil (equation 2) or CO_2 (equation 3) samples, *at% C_{ref}* = the ^{13}C at% of natural abundance control soil (equation 2) or CO_2 (equation 3) samples, *at% label* = the ^{13}C at% of the label solution (5 at %), and *Cumulative $^{12}CO_2$* = the cumulative CO_2 respired over the incubation period (µg CO_2-C g^{-1} dry soil). Respiration data was blank-corrected using empty mason jars that were flushed with CO_2-free air and incubated in parallel with soil samples. The

cumulative $^{13}CO_2$ produced during the 2-week incubation was estimated by first calculating hourly flux rates at four timepoints during the incubation (0-24 h, 24-72 h, 5-7 days, and 12-14 days), and then pairing each of the hourly flux rates with four distinct periods (0-1 days, 1-4 days, 4-8 days, and 8-14 days, respectively). We then estimated the cumulative $^{13}CO_2$ produced by multiplying each hourly flux rate by the number of hours in each paired period and then adding the products. We used this approach to maximize sampling resolution during early stages of the incubation, since preliminary tests showed CO_2 flux rates were more variable at the start of the incubation (0-24 h and 24-72 h) than at the end (8-14 days).

Carbon use efficiency was estimated as:

$$CUE = \frac{^{13}Mic\,C}{^{13}Mic\,C + ^{13}CO_2} \quad (4)$$

$$^{13}Mic\,C = (Chl\,DOC - NChl\,DOC) \times \frac{at\,\%\,Mic\,C_L - at\,\%\,Mic\,C_{ref}}{at\,\%\,label - at\,\%\,Mic\,C_{ref}} \quad (5)$$

$$at\,\%\,Mic\,C = \frac{\left[(at\,\%Chl\,DOC \times Chl\,DOC) - (at\,\%\,NChl\,DOC \times NChl\,DOC)\right]}{(Chl\,DOC - NChl\,DOC)} \quad (6)$$

where *Chl DOC* = the total C of K_2SO_4 extracts fumigated with chloroform, *NChl DOC* = the total C of K_2SO_4 extracts without chloroform, *at% Chl* = the at% of chloroform-fumigated extracts, *at% NChl* = the at% of non-chloroform-fumigated extracts, *at% Mic* C_L = the at% of microbial biomass in labelled samples, and *at% Mic* C_N = the at% of microbial biomass in natural abundance control samples. In some cases, $^{13}Mic\,C$ (equation 5), and thus CUE, could not be calculated because *NChl DOC* was higher than *Chl DOC* (e.g., in the 2-week incubations at GRASS).

Since glucose is typically completely taken up by microbes within a few hours after it is added to soils, the ^{13}C retained in soils in the CSE measurement represents ^{13}C in microbial

biomass and ^{13}C in microbially-produced residues, thought to contribute to long-term soil C storage (Geyer et al., 2020). We measured CSE and CUE in both short- (24 h) and long-term (2 weeks) incubations. The short-term incubation is defined as the microbial community-scale CSE (CSE_C) and CUE (CUE_C), and is thought to closely track the efficiency of the microbial community to incorporate C in microbial products (Geyer et al., 2016). In contrast, the long-term incubation represents ecosystem-scale CSE (CSE_E) and CUE (CUE_E) and integrates microbial community-scale dynamics and the recycling of microbial necromass and residues, and is thus affected by soil organo-mineral interactions (Geyer et al., 2016). We chose 24 h for short-term incubations as it is a widely used incubation time, facilitating comparisons with other studies. We chose two weeks for long-term incubations because preliminary tests showed that the CO_2 pulse after label addition was largely over after two weeks, and thus no significant further partitioning of ^{13}C between soil and atmosphere is expected after that point (Geyer et al., 2020).

We measured CSE and CUE exclusively on beneath shrub samples during the wet season when soils are moist to support microbial communities—summers at our site can extend > 6 months without precipitation, representing a period of significantly decreased decomposition and microbial activity (Schimel 2018a; Aronson et al. 2019). Moreover, due to higher microbial densities, the microbial pump and effects of CSE and CUE are likely more important in soils beneath shrubs than in the interspaces (Sokol and Bradford 2019). Detailed methods used to measure CSE and CUE are included in the Supporting Information.

Statistical analyses

In CHAP and CSS1, we tested for significant N-fertilization treatment effects using three-way mixed ANOVAs with treatment and soil position (beneath shrub vs. interspace) as between-subject factors and season as within-subject factor. If a significant ($p<0.05$) or

marginally significant ($p<0.1$) treatment effect was found, we used two-way ANOVAs to test for significant treatment effects within each season, using treatment and soil position as between-subject factors. If a significant ($p<0.05$) or marginally significant ($p<0.1$) treatment effect was found within either season, we used paired post-hoc t-tests to test for treatment effects within each soil position. P-values in the post-hoc tests were Bonferroni-corrected to account for an increase in type-1 error due to multiple comparisons. We checked for normal distribution of the tested variables using Shapiro-Wilk tests after standardizing and pooling data points from both treatments and ~~soil positions~~ microhabitats (beneath shrubs and in the interspaces between shrubs). Variance homogeneity was evaluated by comparing standard deviations visually. If assumptions were not met, data were log-transformed, square root-transformed, or multiplicative inverse-transformed, in that order. Since at GRASS and CSS2 we only took samples from beneath shrubs, we tested for significant N-fertilization treatment effects using two-way mixed ANOVAs with treatment as between-subject factor and season as within-subject factor. Post-hoc testing, assumption testing, and data transformations were done similarly as for CHAP and CSS1. Since assumptions could not be met for NO_3^- and NH_4^+, three-way and two-way ANOVAs for these variables were performed on aligned rank transformed data (Wobbrock et al. 2011). We treated control and N-fertilized plots as dependent in the post-hoc tests due to the paired plot design at our sites. This allows us to account for landscape-scale variation in soil and plant properties, improving the statistical power at the low sample sizes typical for long-term ecosystem studies. We only tested for treatment effects within each site and not across sites, since each site differs in multiple factors such as fertilizer type, acidification, vegetation, and site.

We constructed a structural equation model (SEM) to test how different soil variables affected POC and MAOC. The variables were selected based on conceptual frameworks of

SOM formation outlined in the introduction and partially illustrated in Fig.1. The SEM was constructed based on maximum-likelihood estimation using the lavaan package in R (Rossel 2012). The data were pooled from all four sites and both seasons (n=96). We tested for multivariate normality of the tested variables using Henze-Zirkler's test. Multivariate normality was still not fulfilled after transformations since soil pH followed a bimodal distribution. Therefore, we used robust standard errors of path coefficients and a Satorra-Bentler scaled maximum-likelihood estimation to account for a potential bias introduced by violating the multivariate normality assumption (Satorra and Bentler 1994; Curran et al. 1996), using the "MLM" function in the lavaan package. Model fit was evaluated by model chi-square statistics, confirmatory factor index, Tucker Lewis index, and root mean square error of approximation. All statistical analyses were performed in R-Studio version 4.1.2 (R Core Team).

Results

Soil organic C fractions

Nitrogen fertilization had no effect on POC at our sites (Fig. 2), but it decreased MAOC (Fig. 3, $p = 0.002$) at the acidified CHAP site; MAOC decreased by 16% across both ~~soil positions~~microhabitats (beneath shrubs and in the interspaces between shrubs) and seasons. This decrease in MAOC at CHAP appeared to be stronger in the wet season than in the dry season (Fig. 3; $p_{adj.} = 0.052$). In contrast to CHAP, N fertilization did not affect MAOC at the other sites, including the CSS1 site that had also been acidified by N fertilization.

Microbial biomass and potential extracellular enzyme activities

N fertilization decreased microbial biomass C by 38% at the acidified CHAP site (Fig. 4, $p = 0.001$) and by 24% at the acidified CSS1 site (Fig. 4, $p = 0.016$), but had no effect on microbial biomass C at the other, unacidified, sites. At CHAP, N fertilization significantly decreased microbial biomass C in both the wet ($p_{adj.} = 0.018$) and the dry season ($p_{adj.} = 0.048$), with this effect trending to be mostly significant in the interspaces relative to beneath shrubs (Fig. 4; $p_{adj.} = 0.098$ for wet season and $p_{adj.} = 0.056$ for dry season). At CSS1, N fertilization decreased microbial biomass C only in the wet season ($p_{adj.} = 0.026$) and only in the interspaces ($p_{adj.} = 0.050$).

Potential activities of all C- and N-acquiring extracellular enzymes decreased significantly with N fertilization at the acidified CHAP and CSS1 sites (Table 4), except for N-acquiring NAG which remained unchanged at CSS1. At CHAP, across both seasons and across ~~soil positions~~microhabitats, AG decreased by 51% ($p < 0.001$), BG by 60% ($p < 0.001$), CBH by 47% ($p < 0.001$), NAG by 51% ($p < 0.001$), LAP by 62% ($p < 0.001$) and PHO by 57% ($p < 0.001$). At CSS1, AG decreased by 47% ($p < 0.001$), BG by 55% ($p < 0.001$), CBH by 48% ($p < 0.001$), LAP by 45% ($p < 0.001$) and PHO by 40% ($p < 0.001$). When we normalized enzyme activity on a per mg microbial biomass basis—to determine whether microbial investment in enzyme production changed—N fertilization did not affect enzyme activities at either site (Supp. Table 1), except for N-acquiring NAG which increased by 60% at CSS1 ($p = 0.033$). In contrast to the acidified sites, N fertilization had no effect on potential soil extracellular enzyme activities at the non-acidified sites GRASS and CSS2 (Table 4).

Carbon stabilization efficiency and ~~carbon~~ C use efficiency

Since we measured CSE and CUE only in soils sampled beneath shrubs during the wet season, we tested for an N fertilization effect on CSE and CUE with paired t-tests. Community-scale CSE (CSE_C), evaluated in the short-term incubations, decreased by 0.13× in all eight N fertilization plots at CHAP and CSS1 relative to the control, but the difference was not significant at CHAP and only marginally significant at CSS1 (Fig. 5, $p = 0.095$). In contrast to CSE_C, N fertilization had no effect on ecosystem-scale CSE (CSE_E) at CSS1, which was evaluated in long-term incubations (Fig. 5). At CSS2, despite no changes in CSE_C, N fertilization marginally increased CSE_E by 0.14× relative to controls ($p = 0.073$). No effects were detected at GRASS.

N fertilization significantly decreased community-scale CUE (CUE_C) by 0.45× at CHAP (Fig. 6, $p = 0.024$) and by 0.25× at CSS1 (Fig. 6, $p = 0.006$) relative to controls. N fertilization also decreased ecosystem-scale CUE (CUE_E) by 0.21× at CHAP ($p = 0.027$) relative to controls. Like CSE, at CSS2, N fertilization had no effect on CUE_C but marginally increased CUE_E by 0.32× relative to controls ($p = 0.073$). No effect was detected at GRASS, where only CUE_C could be calculated.

Soil exchangeable calcium

Long-term N fertilization had no effect on exchangeable Ca in non-acidified sites, but reduced soil exchangeable Ca at acidified sites (Fig. 7); exchangeable Ca decreased by 47% at CHAP ($p < 0.001$) and by 16% at CSS1 ($p = 0.003$) when analyzed across season and across samples beneath shrubs and in the interspaces, albeit with a marginally significant interaction between treatment effect and soil position at CSS1 ($p = 0.051$). At CHAP, N fertilization significantly decreased exchangeable Ca in both the wet ($p_{adj.} = 0.007$) and the dry season ($p_{adj.} = 0.003$). When analyzing the ~~soil positions~~microhabitats individually, only

beneath shrubs during the dry season samples decreased significantly with N fertilization ($p_{adj.}$ = 0.033). At CSS1, N fertilization reduced exchangeable Ca in both seasons ($p_{adj.}$ = 0.022 for wet season and $p_{adj.}$ = 0.001 for dry season). However, there was a significant interaction between the treatment and soil position in the dry season ($p_{adj.}$ = 0.004) where exchangeable Ca decreased only beneath shrubs ($p_{adj.}$ = 0.006). In the wet season, N fertilization significantly decreased exchangeable Ca only in interspaces ($p_{adj.}$ = 0.038).

Controls over soil organic ~~carbon~~ C fractions

The constructed SEM validated the importance of abiotic soil characteristics in driving variation in MAOC (Fig. 8). Soil pH explained 33% of variation in exchangeable Ca across fertilization treatments, sites, seasons, and ~~soil positions~~microhabitats. Together with POC, soil pH and exchangeable Ca explained 45% of variation in microbial biomass. MAOC was strongly and positively affected by exchangeable Ca, which directly and, through its positive effect on microbial biomass, explained 58% of the variation in MAOC. In contrast, variation in POC was not well explained by our chosen soil variables—soil pH and exchangeable Ca only explained 4% of variation in POC—consistent with the fact that N fertilization had no effect at our sites (Fig. 2).

Discussion

We studied changes in soil C fractions in four dryland sites in Southern California that span three dominant vegetation types and have been fertilized with N for more than 13 years. ~~long-term N fertilization experiments where t~~Two sites (CHAP and CSS1) were fertilized with urea, NH_4^+, and NO_3^-, and strongly acidified, whereas the other two sites (GRASS and CSS2) were fertilized with $CaNO_3$ to prevent acidification. Fertilization had no effects on soil C fractions, except for at one site, where the mineral-associated organic C fraction (MAOC) decreased likely because of changes in soil physicochemical properties induced by

acidification. Contrary to previous studies, particulate organic C (POC) did not increase despite above-ground biomass increasing in three of the four study systems (Parolari et al. 2012; Vourlitis et al. 2021a) coupled to a likely decrease in biotic decomposition in soil—soil microbial biomass and extracellular enzyme activities decreased—in the two sites that experienced strong acidification. Furthermore, we found no evidence for a microbial ~~carbon-~~ C pump governing the persistence of soil C under N enrichment in these drylands; long-term but not short-term CUE and CSE increased in one of the non-acidified sites but did not lead to changes in MAOC. Importantly, however, we observed significant losses of MAOC at the acidified CHAP site, likely because of pH-induced Ca loss that destabilized organo-mineral interactions. Our measurements suggest that long-term effects of N fertilization on dryland C storage are of abiotic nature, such that drylands where Ca-stabilization of SOC is prevalent may be most at risk for significant MAOC losses.

Particulate organic C (POC) dynamics

We hypothesized N fertilization would increase POC due to increased plant biomass production ~~and, therefore, POC~~ as observed in ~~other drylands~~semi-arid grasslands in China (Ye et al. 2018) and Mediterranean grasslands in California (Lin et al. 2019). However, despite N fertilization increasing above-ground plant biomass at CHAP, CSS1, and GRASS (data for CSS2 are not available) (Parolari et al. 2012; Vourlitis et al. 2021), POC did not increase. It is possible that N fertilization could have increased microbial respiration of plant C inputs, preventing POC accumulation in soils (Knorr et al. 2005; Khan et al. 2007; Finn et al. 2015), but this is unlikely at our sites. This is because although adding N increased litter quality at GRASS (Allison et al. 2013), neither litter decomposition rates (Allison et al. 2013) nor soil microbial respiration rates increased (measured in CUE incubations; Supp. Fig. 1). Furthermore, N fertilization is predicted to stimulate microbial decomposition only if pH

remains relatively constant (Averill and Waring 2018), but CHAP and CSS1 experienced strong acidification, decreasing both soil microbial biomass and hydrolytic soil extracellular enzymes—putative proxies signaling high potential for organic matter decomposition. Indeed, soil microbial respiration rates (measured in CUE incubations only in wet season and only beneath shrubs) decreased by 61% in fertilized plots at CHAP ($p = 0.088$) and not significantly in CSS1 (Supp. Fig. 1). This is in line with findings from semi-arid grasslands in China, where N fertilization led to soil acidification together with decreases in microbial biomass and soil respiration (Chen et al. 2016). While no data on litter decomposition rates exist, the strong decrease in soil microbial biomass and almost all potential soil hydrolytic enzyme activities, suggests that microbial soil organic matter decomposition was suppressed in acidified sites, which in other studies has typically increased ~~in~~ POC (Treseder 2008; Zak et al. 2019). Therefore, other processes are likely preventing POC from building up in these drylands.

The fact that increased aboveground biomass production did not lead to increases in POC could mean that roots are more important for building POC at our sites. It is well established that aboveground litter in drylands can degrade photochemically before being incorporated in the soil, independent of litter and soil properties (Austin and Vivanco 2006). In some dryland soils this suggests aboveground litter contributes little to soil organic C, and that root biomass contributes most to POC (e.g., Berenstecher et al. 2021). Therefore, the response of POC to N deposition may depend more on changes in root production. Indeed, a fertilization study in a semi-arid grassland found POC increased together with root biomass (Ye et al. 2018). While root data is not available for GRASS and CSS2, cumulative root production was unchanged after the first 15 years of fertilization at CHAP and CSS1 (Vourlitis et al. 2021a), potentially explaining why POC did not change despite increases in

aboveground biomass. Overall, our data suggest that increased above-ground biomass production is decoupled from POC at our sites, and that POC may be more affected by root production.

In addition to aboveground decomposition, POC may have not increased at our sites because the effects of N fertilization may be confounded by annual changes in plant biomass production and decomposition in response to precipitation. Precipitation strongly affects plant biomass production and its response to N fertilization in drylands (Yahdjian et al. 2011; Hou et al. 2021), with several studies showing N fertilization increased plant production only under experimental water addition (Ma et al. 2020) or in years with above-average precipitation (Hall et al. 2011; Ladwig et al. 2012; Vourlitis 2012; Su et al. 2013). Similarly, dryland soils can experience high seasonal and year-to-year variation in SOC (Hou et al. 2021). The strong seasonal changes we observed in POC from the dry to the wet season (+47% for POC and only -5% for MAOC, Fig. 2 and Fig. 3) suggest that much of the seasonal variation in SOC (+13% in our study, Table 2) observed in drylands is driven by changes in POC, which is considered a more dynamic pool than MAOC (Lavallee et al. 2020). Furthermore, wind, water, and faunal activity can horizontally and vertically transport litter and POC from where it has been produced (Throop and Belnap 2019). Therefore, seasonal changes might make it challenging to detect differences in POC and, by extension, in SOC. For example, SOC at CHAP and CSS1 responded negatively, positively, or not at all to N fertilization depending on the year of measurement (Vourlitis et al. 2021b), while another study found increases in SOC at CSS2 in 2012 where we found no changes (Khalili et al. 2016). Overall, even if differences in POC may have been detected in some years, the observed dynamic nature of POC suggests that much of the POC in our study may turn over relatively fast, with only a small fraction contributing to long-term C storage.

Microbial C use and stabilization efficiency

We found limited evidence (i.e., changes in CSE or MAOC) for an acceleration of the microbial C pump under N fertilization in the non-acidified sites at GRASS and CSS2. It has been suggested that if soils have a high enough sorption potential and do not acidify, N fertilization should alleviate microbial N limitation, increasing microbial CUE and, thereby, MAOC (Manzoni et al. 2012b; Averill and Waring 2018; Poeplau et al. 2019). While we found no changes in short-term CUE or CSE at GRASS or CSS2, long-term CUE and CSE increased at CSS2, but without increasing MAOC. Short-term CUE and CSE are mostly regulated by microbial community physiological responses, whereas long-term incubations also include effects of organo-mineral interactions and recycling of C exudates (Geyer et al. 2016). The lack of a response to N fertilization in short-term incubations could indicate that, in drylands, microbes may be instead mostly limited by water and C availability (Schaeffer et al. 2003; Homyak et al. 2018; Schimel 2018b). Alternatively, microbial CUE can also change in response to changes in microbial community composition (Li et al. 2021). While microbial community composition changed at GRASS (Amend et al. 2016), the changes may not have been directed enough to favor microbes with a higher CSE (Pold et al. 2020). Thus, the increase in long-term, but not short-term CUE and CSE in fertilized plots at CSS2 suggests more efficient recycling of C compounds (Geyer et al. 2016), which after more than ten years of N fertilization has not led to detectable changes in MAOC. Overall, N fertilization did not increase dryland C storage through changes in microbial CUE or CSE.

It is possible we did not detect an acceleration of the microbial C pump under N fertilization because the low sorption potential of soils at our sites inhibits the microbial in-vivo pathway of C stabilization (Liang et al. 2017; Islam et al. 2022). For example, short-term CSE decreased in all N deposition plots at CHAP and CSS1 but had no effect on long-

term CSE. The fact that short- and long-term CUE decreased in all N deposition plots at CHAP and CSS1 suggests that microbial community changes and microbial stress in response to acidification could have accounted for the decrease in short-term CSE at CHAP and CSS1 (Lauber et al. 2009; Jones et al. 2019; Grant et al. 2022). However, the fact that the initial differences in CSE did not translate into long-term stabilization means that the additional C that was initially retained in control plots was later recycled and respired over the course of the long-term incubation (Geyer et al. 2016, 2020). Similar to a previous study on low-sorption sandy soils (Creamer et al. 2014), this could indicate that the C stabilization potential in the studied soils is too low, so that even if microbes initially retain C more efficiently, there is no viable mechanism for long-term storage (Islam et al. 2022)—the soils may be operating at or near their capacity to store C. Therefore, it is unlikely that N addition would affect C stabilization at our site via the microbial C pump, as microbial C accumulation efficiency may strongly depend on soil mineralogy (Cai et al. 2022).

~~M~~Changes in mineral-associated organic C (MAOC)

We found significant MAOC losses in response to N fertilization at CHAP; N fertilization lowered MAOC by 13% in the dry season and by 21% in the wet season relative to control plots (Fig. 3). MAOC losses in drylands have been observed before and linked to increased decomposition related to changes in microbial physiology (Lin et al. 2019) and/or acidification (Ye et al. 2018). However, an increase in MAOC decomposition rates at our site due to changes in microbial physiology is unlikely since biotic decomposition likely decreased at CHAP as we discussed earlier for POC. Furthermore, the fact that the decrease in MAOC was also observed in the interspaces between shrubs, where we found significantly lower microbial biomass, points to acidification as the likely driver behind the MAOC decrease, not changes in microbial physiology.

Acidification can decrease MAOC by destabilizing Ca–organic C associations that make the C accessible to microbes or vulnerable to loss via dissolved organic ~~carbon~~ C (Bailey et al. 2019). Polyvalent cations such as Ca are important in bridging negatively charged C compounds to negatively charged mineral surfaces, particularly in dryland soils (Rasmussen et al. 2018; Rowley et al. 2018). Even though we did not measure Ca–organic C pools directly, exchangeable Ca was strongly correlated with MAOC and significantly decreased at CHAP (Fig. 6), suggesting that Ca loss is the main pathway for MAOC loss at our sites. This is consistent with results from nine temperate grasslands across the United States where soil texture and mineralogy were key predictors of SOC more so than N fertilization (Keller et al. 2022), suggesting that N-induced acidification can directly affect soil physical factors that control MAOC. ~~Furthermore, t~~This mechanism was further supported by our SEM, highlighting that MAOC was correlated with exchangeable Ca, which both directly, and indirectly through microbial biomass, explained 58% of the variation in MAOC (Fig. 8). Our findings are also consistent with ~~several~~ studies in mesic agricultural systems (Wan et al. 2021) and semi-arid grasslands in China (Ye et al. 2018) reporting losses in Ca-associated organic matter in response to N-induced acidification ~~(Ye et al. 2018; Wan et al. 2021)~~, suggesting MAOC loss was primarily related to pH-induced destabilization of Ca–organic C associations.

While a loss of Ca-associated organic matter can explain the loss of MAOC at our CHAP site, we found that strong acidification and loss of exchangeable Ca did not decrease MAOC at CSS1. On average the finer- textured (see Supp. Table 2 for texture) CSS1 lost less Ca than the coarser-textured CHAP (16% vs. 47%) and had higher baseline Ca levels (1.6 mg g^{-1} at CSS1 averaged across ~~soil positions~~microhabitats and seasons in control plots vs. 0.8 mg g^{-1} at CHAP), perhaps suggesting that there is a threshold beyond which decreases in

exchangeable Ca destabilize cation bridges and Ca-associated organic matter. However, we found that out of the sixteen studied N addition cases at CSS1 (4 plots × 2 seasons × 2 ~~soil positions~~microhabitats), six did not decrease in MAOC. Four of these six cases come from two plots at CSS1 which experienced significant dieback of native shrub vegetation and replacement by invasive forbs (George Vourlitis, personal communication). It is possible that a change to a faster cycling grass- and forb-dominated vegetation system with higher root biomass and turnover overrode potential Ca-related C losses and led to C accumulation in these plots (Qi et al. 2019; Sokol and Bradford 2019); strong increases in SOC upon CSS invasion by grasses have been observed before (Wolkovich et al. 2010). Since N enrichment is expected to shift plant community composition (Plaza et al. 2018a), particularly in CSS (Kimball et al. 2014; Valliere et al. 2017), future studies on how effects of vegetation change on SOC fractions might interact with direct effects of N addition are warranted.

Implications for N deposition effects on C storage in drylands

Given the high seasonal fluctuation in SOC and POC in drylands (this study; Hou et al. 2021a; Vourlitis et al. 2021b), the consistently observed MAOC losses at CHAP could be the first sign for a future decrease in C storage in soils prone to acidification. Notably, even more alkaline soils considered to be better buffered against pH changes than soils in our study can acidify if enough N has been added (Yang et al. 2012; Tian and Niu 2015). If acidification occurs, Ca leaching and concurrent C losses may be mostly restricted to topsoils in areas in which Ca-associations make up an important fraction of C stabilization (Niu et al. 2021), although data is limited. While there is currently no good understanding of the distribution of Ca-associated organic C pools, correlation studies suggest that Ca is particularly important for C stabilization in drylands above pH 6.5 and dominated by 2:1 phyllosilicates (Rasmussen et al. 2018). Potential decreases in topsoil C in these areas could

have important consequences for soil structure, water holding capacity, and soil fertility. Notably, inputs of above-ground biomass might not help to balance these losses if above-ground litter does not build up in soils as we and others observed (Berenstecher et al. 2021), particularly since root biomass does not always increase in response to N enrichment (Kummerow et al. 1982; Zeng et al. 2010; Ladwig et al. 2012; Vourlitis et al. 2021a). Furthermore, the form of N deposited, either as NH_4^+ or NO_3^-, can affect soil acidification (Tian and Niu 2015). While NH_3 emission can initially buffer acidity in precipitation, once deposited, NH_4^+ can still cause acidification depending on whether it is taken up by plants or nitrified (Rodhe et al. 2002). Nitrification produces 2 H^+ ions and NO_3^-, and the NO_3^- can then co-leach as a companion anion to base cations enriching sites with H^+ (Rodhe et al. 2002). Since a global shift from NO_3^- to NH_3 deposition is expected (Lamarque et al. 2013; Kanakidou et al. 2016), future studies should focus specifically on how the deposition and consumption pathways of these compounds affect acidification and C dynamics in drylands.

Conclusion

We sampled soils at four long-term N-fertilization sites to understand how increasing rates of atmospheric N deposition may affect SOC dynamics in drylands. In contrast to studies from forest soils where N enrichment decreases microbial biomass, extracellular enzyme activity, and respiration with a concomitant increase in SOC (Treseder 2008; Janssens et al. 2010; Riggs and Hobbie 2016; O'Sullivan et al. 2019), we found that N enrichment had relatively small effects on SOC storage, with no C accumulating in these dryland soils despite non-acidic conditions that were expected to build SOC via the microbial C pump (Liang et al. 2017; Averill and Waring 2018). However, in soils experiencing strong N-induced acidification, we observed substantial Ca losses that destabilized MAOC in one of the sites. As soils saturate with N (Homyak et al. 2014), our measurements highlight a pH-

dependent mechanism whereby Ca-stabilization of SOC in drylands may decrease, leading to a loss of SOC. Overall, microbial processes in dryland soils may be ultimately governed by C and water availability, suggesting that N enrichment is unlikely to benefit SOC, and instead favor decreases in SOC as a result of decalcification of the soil and destabilization of MAOC.

Acknowledgments

We thank reserve managers at Santa Margarita and Sky Oaks ecological reserves, and the Irvine Ranch Conservancy for access to research sites. We thank Dr. Kevin Geyer for assistance with the CUE method and Dr. Gabriela Mendoza for artwork design. This research was supported by the United States National Science Foundation (award DEB 1916622 to PMH, EJH, ELA, and JPS) and the US Department of Energy, Office of Science, BER award DE-SC0020382 to SDA.

References

Allison SD, Lu Y, Weihe C, et al (2013) Microbial abundance and composition influence litter decomposition response to environmental change. Ecology 94:714–725. doi: 10.1890/12-1243.1

Amend AS, Martiny AC, Allison SD, et al (2016) Microbial response to simulated global change is phylogenetically conserved and linked with functional potential. ISME Journal 10:109–118. doi: 10.1038/ismej.2015.96

Aronson EL, Goulden ML, Allison SD (2019) Greenhouse gas fluxes under drought and nitrogen addition in a Southern California grassland. Soil Biology and Biochemistry 131:19–27. doi: 10.1016/j.soilbio.2018.12.010

Austin AT, Vivanco L (2006) Plant litter decomposition in a semi-arid ecosystem controlled

679 by photodegradation. Nature 442:555–558. doi: 10.1038/nature05038
680 Averill C, Waring B (2018) Nitrogen limitation of decomposition and decay: How can it
681 occur? Global Change Biology 24:1417–1427. doi: 10.1111/gcb.13980
682 Bailey VL, Pries CH, Lajtha K (2019) What do we know about soil carbon destabilization?
683 Environmental Research Letters 14:083004
684 Barbour KM, Weihe C, Allison SD, Martiny JBH (2022) Bacterial community response to
685 environmental change varies with depth in the surface soil. Soil Biology and
686 Biochemistry 172:108761. doi: 10.1016/j.soilbio.2022.108761
687 Berenstecher P, Araujo PI, Austin AT (2021) Worlds apart: Location above- or below-ground
688 determines plant litter decomposition in a semi-arid Patagonian steppe. Journal of
689 Ecology 109:2885–2896. doi: 10.1111/1365-2745.13688
690 Bradford MA, Keiser AD, Davies CA, et al (2013) Empirical evidence that soil carbon
691 formation from plant inputs is positively related to microbial growth. Biogeochemistry
692 113:271–281. doi: 10.1007/s10533-012-9822-0
693 Brookes PC, Landman A, Pruden G, Jenkinson DS (1985) Chloroform fumigation and the
694 release of soil nitrogen: A rapid direct extraction method to measure microbial biomass
695 nitrogen in soil. Soil Biology and Biochemistry 17:837–842. doi: 10.1159/000477898
696 Burns RG, DeForest JL, Marxsen J, et al (2013) Soil enzymes in a changing environment:
697 Current knowledge and future directions. Soil Biology and Biochemistry 58:216–234.
698 doi: 10.1016/j.soilbio.2012.11.009
699 Butcher KR, Nasto MK, Norton JM, Stark JM (2020) Physical mechanisms for soil moisture
700 effects on microbial carbon-use efficiency in a sandy loam soil in the western United
701 States. Soil Biology and Biochemistry 150:107969. doi: 10.1016/j.soilbio.2020.107969
702 Cai Y, Ma T, Wang Y, et al (2022) Assessing the accumulation efficiency of various

703 microbial carbon components in soils of different minerals. Geoderma 407:115562. doi:
704 10.1016/j.geoderma.2021.115562
705 Castellano MJ, Mueller KE, Olk DC, et al (2015) Integrating plant litter quality , soil organic
706 matter stabilization , and the carbon saturation concept. Global Change Biology
707 21:3200–3209. doi: 10.1111/gcb.12982
708 Chen D, Li J, Lan Z, et al (2016) Soil acidification exerts a greater control on soil respiration
709 than soil nitrogen availability in grasslands subjected to long-term nitrogen enrichment.
710 Functional Ecology 30:658–669. doi: 10.1111/1365-2435.12525
711 Cotrufo MF, Ranalli MG, Haddix ML, et al (2019) Soil carbon storage informed by
712 particulate and mineral-associated organic matter. Nature Geoscience 12:989–994. doi:
713 10.1038/s41561-019-0484-6
714 Creamer CA, Jones DL, Baldock JA, et al (2016) Is the fate of glucose-derived carbon more
715 strongly driven by nutrient availability, soil texture, or microbial biomass size? Soil
716 Biology and Biochemistry 103:201–212. doi: 10.1016/j.soilbio.2016.08.025
717 Creamer CA, Jones DL, Baldock JA, Farrell M (2014) Stoichiometric controls upon low
718 molecular weight carbon decomposition. Soil Biology and Biochemistry 79:50–56. doi:
719 10.1016/j.soilbio.2014.08.019
720 Curran PJ, West SG, Finch JF (1996) The robustness of test statistics to nonnormality and
721 specification error in confirmatory factor analysis. Psychological Methods 1:16–29
722 Deng L, Huang C, Shangguan DKZ, et al (2020) Soil GHG fluxes are altered by N
723 deposition : New data indicate lower N stimulation of the N2O flux and greater
724 stimulation of the calculated C pools. Global Change Biology 26:2613–2629. doi:
725 10.1111/gcb.14970
726 Fenn ME, Allen EB, Weiss SB, et al (2010) Nitrogen critical loads and management

727 alternatives for N-impacted ecosystems in California. Journal of Environmental
728 Management 91:2404–2423. doi: 10.1016/j.jenvman.2010.07.034
729 Fierer N (2003) Stress ecology and the dynamics of microbial communities and processes in
730 soil. ProQuest Dissertations Publishing, University of California, Santa Barbara
731 Finn D, Page K, Catton K, et al (2015) Effect of added nitrogen on plant litter decomposition
732 depends on initial soil carbon and nitrogen stoichiometry. Soil Biology and
733 Biochemistry 91:160–168. doi: 10.1016/j.soilbio.2015.09.001
734 Geyer K, Schnecker J, Grandy AS, et al (2020) Assessing microbial residues in soil as a
735 potential carbon sink and moderator of carbon use efficiency. Biogeochemistry 4:237–
736 249. doi: 10.1007/s10533-020-00720-4
737 Geyer KM, Kyker-snowman E, Grandy AS, Frey SD (2016) Microbial carbon use efficiency:
738 accounting for population, community, and ecosystem-scale controls over the fate of
739 metabolized organic matter. Biogeochemistry 127:173–188. doi: 10.1007/s10533-016-
740 0191-y
741 Grant T, Sethuraman A, Escobar MA, Vourlitis GL (2022) Chronic dry nitrogen inputs alter
742 soil microbial community composition in Southern California semi-arid shrublands.
743 Applied Soil Ecology 176:104496. doi: 10.1016/j.apsoil.2022.104496
744 Gruber N, Galloway JN (2008) An Earth-system perspective of the global nitrogen cycle.
745 Nature 451:293–296. doi: 10.1038/nature06592
746 Hall SJ, Sponseller RA, Grimm NB, et al (2011) Ecosystem response to nutrient enrichment
747 across an urban airshed in the Sonoran Desert. Ecological Applications 21:640–660. doi:
748 10.1890/10-0758.1
749 Harpole SW, Potts DL, Suding KN (2007) Ecosystem responses to water and nitrogen
750 amendment in a California grassland. Global Change Biology 13:2341–2348. doi:

751 10.1111/j.1365-2486.2007.01447.x
752 Hendershot WH, Duquette M (1986) A simple barium chloride method for determining
753 cation exchange capacity and exchangeable cations. Soil Science Society of America
754 Journal 50:605–608. doi: 10.2136/sssaj1986.03615995005000030013x
755 Homyak PM, Blankinship JC, Slessarev EW, et al (2018) Effects of altered dry season length
756 and plant inputs on soluble soil carbon. Ecology 99:2348–2362. doi: 10.1002/ecy.2473
757 Homyak PM, Sickman JO, Miller AE, et al (2014) Assessing Nitrogen-Saturation in a
758 Seasonally Dry Chaparral Watershed: Limitations of Traditional Indicators of N-
759 Saturation. Ecosystems 17:1286–1305. doi: 10.1007/s10021-014-9792-2
760 Hou E, Rudgers JA, Collins SL, et al (2021) Sensitivity of soil organic matter to climate and
761 fire in a desert grassland. Biogeochemistry 156:59–74. doi: 10.1007/s10533-020-00713-
762 3
763 Islam MR, Singh B, Dijkstra FA (2022) Stabilisation of soil organic matter : interactions
764 between clay and microbes. Biogeochemistry 160:145–158. doi: 10.1007/s10533-022-
765 00956-2
766 Janssens IA, Dieleman W, Luyssaert S, et al (2010) Reduction of forest soil respiration in
767 response to nitrogen deposition. Nature Geoscience 3:315–322. doi: 10.1038/ngeo844
768 Jones DL, Cooledge EC, Hoyle FC, et al (2019) pH and exchangeable aluminum are major
769 regulators of microbial energy flow and carbon use efficiency in soil microbial
770 communities. Soil Biology and Biochemistry 138:107584. doi:
771 10.1016/j.soilbio.2019.107584
772 Kanakidou M, Myriokefalitakis S, Daskalakis N, et al (2016) Past, present, and future
773 atmospheric nitrogen deposition. Journal of the Atmospheric Sciences 73:2039–2047.
774 doi: 10.1175/JAS-D-15-0278.1

Keller AB, Borer ET, Collins SL, et al (2022) Soil carbon stocks in temperate grasslands differ strongly across sites but are insensitive to decade-long fertilization. Global Change Biology 28:1659–1677. doi: 10.1111/gcb.15988

Khalili B, Ogunseitan OA, Goulden ML, Allison SD (2016) Interactive effects of precipitation manipulation and nitrogen addition on soil properties in California grassland and shrubland. Applied Soil Ecology 107:144–153. doi: 10.1016/j.apsoil.2016.05.018

Khan SA, Mulvaney RL, Ellsworth TR, Boast CW (2007) The myth of nitrogen fertilization for soil carbon sequestration. Journal of Environmental Quality 36:1821–1832. doi: 10.2134/jeq2007.0099

Kimball S, Goulden ML, Suding KN, Parker S (2014) Altered water and nitrogen input shifts succession in a southern California coastal sage community. Ecological Applications 24:1390–1404. doi: 10.1890/13-1313.1

Knorr M, Frey SD, Curtis PS (2005) Nitrogen additions and litter decomposition: A meta-analysis. Ecology 86:3252–3257. doi: 10.1890/05-0150

Kummerow J, Avila G, Aljaro M-E, et al (1982) Effect of fertilizer on fine root density and shoot growth in Chilean matorral. Botanical Gazette 143:498–504

Ladwig LM, Collins SL, Swann AL, et al (2012) Above- and belowground responses to nitrogen addition in a Chihuahuan Desert grassland. Oecologia 169:177–185. doi: 10.1007/s00442-011-2173-z

Lamarque JF, Dentener F, McConnell J, et al (2013) Multi-model mean nitrogen and sulfur deposition from the atmospheric chemistry and climate model intercomparison project (ACCMIP): Evaluation of historical and projected future changes. Atmospheric Chemistry and Physics 13:7997–8018. doi: 10.5194/acp-13-7997-2013

Lauber CL, Hamady M, Knight R, Fierer N (2009) Pyrosequencing-based assessment of soil pH as a predictor of soil bacterial community structure at the continental scale. Applied and Environmental Microbiology 75:5111–5120. doi: 10.1128/AEM.00335-09

Lavallee JM, Soong JL, Cotrufo MF (2020) Conceptualizing soil organic matter into particulate and mineral - associated forms to address global change in the 21st century. Global Change Biology 26:261–273. doi: 10.1111/gcb.14859

Li J, Sang C, Yang J, et al (2021) Stoichiometric imbalance and microbial community regulate microbial elements use efficiencies under nitrogen addition. Soil Biology and Biochemistry 156:108207. doi: 10.1016/j.soilbio.2021.108207

Liang C, Schimel JP, Jastrow JD (2017) The importance of anabolism in microbial control over soil carbon storage. Nature Microbiology 2:17105. doi: 10.1038/nmicrobiol.2017.105

Lin Y, Slessarev EW, Yehl ST, et al (2019) Long-term nutrient fertilization increased soil carbon storage in California grasslands. Ecosystems 22:754–766. doi: 10.1007/s10021-018-0300-y

Ma Q, Liu X, Li Y, et al (2020) Nitrogen deposition magnifies the sensitivity of desert steppe plant communities to large changes in precipitation. Journal of Ecology 108:598–610. doi: 10.1111/1365-2745.13264

Maestre FT, Eldridge DJ, Soliveres S, et al (2016) Structure and Functioning of Dryland Ecosystems in a Changing World. Annual Review of Ecology, Evolution, and Systematics 47:215–237. doi: 10.1146/annurev-ecolsys-121415-032311

Manzoni S, Taylor P, Richter A, et al (2012a) Environmental and stoichiometric controls on microbial carbon-use efficiency in soils. New Phytologist 196:79–91. doi: 10.1111/j.1469-8137.2012.04225.x

823 Manzoni S, Taylor P, Richter A, et al (2012b) Environmental and stoichiometric controls on
824 microbial carbon-use efficiency in soils. New Phytologist 196:79–91. doi:
825 10.1111/j.1469-8137.2012.04225.x
826 Marx M-C, Wood M, Jarvis SC (2001) A microplate fluorimetric assay for the study of
827 enzyme diversity in soils. Soil Biology and Biochemistry 33:1633–1640
828 Niu G, Wang R, Hasi M, et al (2021) Availability of soil base cations and micronutrients
829 along soil profile after 13-year nitrogen and water addition in a semi-arid grassland.
830 Biogeochemistry 152:223–236. doi: 10.1007/s10533-020-00749-5
831 O'Sullivan M, Spracklen D V., Batterman SA, et al (2019) Have synergies between nitrogen
832 deposition and atmospheric CO2 driven the recent enhancement of the terrestrial carbon
833 sink? Global Biogeochemical Cycles 33:163–180. doi: 10.1029/2018GB005922
834 Ochoa-hueso R, Maestre FT, Ríos ADL, et al (2013) Nitrogen deposition alters nitrogen
835 cycling and reduces soil carbon content in low-productivity semiarid Mediterranean
836 ecosystems. Environmental Pollution 179:185–193. doi: 10.1016/j.envpol.2013.03.060
837 Osborne BB, Bestelmeyer BT, Currier CM, et al (2022) The consequences of climate change
838 for dryland biogeochemistry. New Phytologist 236:15–20. doi: 10.1111/nph.18312
839 Parolari AJ, Goulden ML, Bras RL (2012) Fertilization effects on the ecohydrology of a
840 southern California annual grassland. Geophysical Research Letters 39:L08405. doi:
841 10.1029/2012GL051411
842 Plaza C, Gascó G, Méndez AM, et al (2018a) Soil Organic Matter in Dryland Ecosystems.
843 Elsevier Inc.
844 Plaza C, Zaccone C, Sawicka K, et al (2018b) Soil resources and element stocks in drylands
845 to face global issues. Scientific Reports 8:13788. doi: 10.1038/s41598-018-32229-0
846 Poeplau C, Don A, Six J, et al (2018) Isolating organic carbon fractions with varying turnover

847 rates in temperate agricultural soils – A comprehensive method comparison. Soil
848 Biology and Biochemistry 125:10–26. doi: 10.1016/j.soilbio.2018.06.025
849 Poeplau C, Helfrich M, Dechow R, et al (2019) Increased microbial anabolism contributes to
850 soil carbon sequestration by mineral fertilization in temperate grasslands. Soil Biology
851 and Biochemistry 130:167–176. doi: 10.1016/j.soilbio.2018.12.019
852 Pold G, Domeignoz-Horta LA, Morrison EW, et al (2020) Carbon use efficiency and its
853 temperature sensitivity covary in soil bacteria. mBio 11:e02293-19. doi:
854 10.1128/mBio.02293-19
855 Potts DL, Suding KN, Winston GC, et al (2012) Ecological effects of experimental drought
856 and prescribed fire in a southern California coastal grassland. Journal of Arid
857 Environments 81:59–66. doi: 10.1016/j.jaridenv.2012.01.007
858 Prăvălie R (2016) Drylands extent and environmental issues. A global approach. Earth-
859 Science Reviews 161:259–278. doi: 10.1016/j.earscirev.2016.08.003
860 Qi Y, Wei W, Chen C, Chen L (2019) Plant root-shoot biomass allocation over diverse
861 biomes: A global synthesis. Global Ecology and Conservation 18:e00606. doi:
862 10.1016/j.gecco.2019.e00606
863 Rasmussen C, Heckman K, Wieder WR, et al (2018) Beyond clay : towards an improved set
864 of variables for predicting soil organic matter content. Biogeochemistry 137:297–306.
865 doi: 10.1007/s10533-018-0424-3
866 Riggs CE, Hobbie SE (2016) Mechanisms driving the soil organic matter decomposition
867 response to nitrogen enrichment in grassland soils. Soil Biology and Biochemistry
868 99:54–65. doi: 10.1016/j.soilbio.2016.04.023
869 Rodhe H, Dentener F, Schulz M (2002) The global distribution of acidifying wet deposition.
870 Environmental Science and Technology 36:4382–4388. doi: 10.1021/es020057g

871 Rossel Y (2012) lavaan: an R package for structural equation modeling. Journal of Statistical
872 Software 48:1–36
873 Rossi LMW, Mao Z, Merino-Martín L, et al (2020) Pathways to persistence: plant root traits
874 alter carbon accumulation in different soil carbon pools. Plant and Soil 452:457–478.
875 doi: 10.1007/s11104-020-04469-5
876 Rowley MC, Grand S, Verrecchia ÉP (2018) Calcium-mediated stabilisation of soil organic
877 carbon. Biogeochemistry 137:27–49. doi: 10.1007/s10533-017-0410-1
878 Satorra A, Bentler PM (1994) Corrections to test statistics and standard errors in covariance
879 structure analysis. In: Latent variables analysis: Applications for developmental
880 research. Sage Publications, Inc, Thousand Oaks, CA, US, pp 399–419
881 Schaeffer SM, Billings SA, Evans RD (2003) Responses of soil nitrogen dynamics in a
882 Mojave Desert ecosystem to manipulations in soil carbon and nitrogen availability.
883 Oecologia 134:547–553. doi: 10.1007/s00442-002-1130-2
884 Schimel JP (2018a) Life in Dry Soils: Effects of Drought on Soil Microbial Communities and
885 Processes. Annual Review of Ecology, Evolution, and Systematics 49:409–432. doi:
886 10.1146/annurev-ecolsys-110617-062614
887 Schimel JP (2018b) Life in dry soils: Effects of drought on soil microbial communities and
888 processes. Annual Review of Ecology, Evolution, and Systematics 49:409–432. doi:
889 10.1146/annurev-ecolsys-110617-062614
890 Slessarev EW, Lin Y, Bingham NL, et al (2016) Water balance creates a threshold in soil pH
891 at the global scale. Nature 540:567–569. doi: 10.1038/nature20139
892 Sokol NW, Bradford MA (2019) Microbial formation of stable soil carbon is more efficient
893 from belowground than aboveground input. Nature Geoscience 12:46–53. doi:
894 10.1038/s41561-018-0258-6

Sokol NW, Sanderman J, Bradford MA (2019) Pathways of mineral - associated soil organic matter formation : Integrating the role of plant carbon source , chemistry , and point of entry. Global Change Biology 25:12–24. doi: 10.1111/gcb.14482

Soong JL, Cotrufo MF (2015) Annual burning of a tallgrass prairie inhibits C and N cycling in soil, increasing recalcitrant pyrogenic organic matter storage while reducing N availability. Global Change Biology 21:2321–2333. doi: 10.1111/gcb.12832

Spohn M, Pötsch EM, Eichorst SA, et al (2016) Soil microbial carbon use efficiency and biomass turnover in a long-term fertilization experiment in a temperate grassland. Soil Biology and Biochemistry 97:168–175. doi: 10.1016/j.soilbio.2016.03.008

Su J, Li X, Li X, Feng L (2013) Effects of additional N on herbaceous species of desertified steppe in arid regions of China: A four-year field study. Ecological Research 28:21–28. doi: 10.1007/s11284-012-0994-9

Throop HL, Belnap J (2019) Connectivity dynamics in dryland litter cycles: Moving decomposition beyond spatial stasis. BioScience 69:602–614. doi: 10.1093/biosci/biz061

Tian D, Niu S (2015) A global analysis of soil acidification caused by nitrogen addition. Environmental Research Letters 10:024019. doi: 10.1088/1748-9326/10/2/024019

Treseder KK (2008) Nitrogen additions and microbial biomass: A meta-analysis of ecosystem studies. Ecology Letters 11:1111–1120. doi: 10.1111/j.1461-0248.2008.01230.x

Valliere JM, Irvine IC, Santiago L, Allen EB (2017) High N , dry : Experimental nitrogen deposition exacerbates native shrub loss and nonnative plant invasion during extreme drought. Global Change Biology 23:4333–4345. doi: 10.1111/gcb.13694

Vance ED, Brookes PC, Jenkinson DS (1987) An extraction method for measuring soil

919 microbial biomass C. Soil Biology and Biochemistry 19:703–707. doi: 10.1016/0038-
920 0717(87)90052-6
921 Vourlitis GL (2012) Aboveground net primary production response of semi-arid shrublands
922 to chronic experimental dry-season N input. Ecosphere 3:Aritcle 22
923 Vourlitis GL, Jaureguy J, Marin L, Rodriguez C (2021a) Shoot and root biomass production
924 in semi-arid shrublands exposed to long-term experimental N input. Science of the Total
925 Environment 754:142204. doi: 10.1016/j.scitotenv.2020.142204
926 Vourlitis GL, Kirby K, Vallejo I, et al (2021b) Potential soil extracellular enzyme activity is
927 altered by long-term experimental nitrogen deposition in semiarid shrublands. Applied
928 Soil Ecology 158:103779. doi: 10.1016/j.apsoil.2020.103779
929 Wan D, Ma M, Peng N, et al (2021) Effects of long-term fertilization on calcium-associated
930 soil organic carbon: Implications for C sequestration in agricultural soils. Science of the
931 Total Environment 772:145037. doi: 10.1016/j.scitotenv.2021.145037
932 Weil RR, Brady NC (2017) The Nature and Properties of Soils, 15th edn. Pearson Education
933 Limited, Essex, England
934 Whalen ED, Grandy AS, Sokol NW, et al (2022) Clarifying the evidence for microbial- and
935 plant-derived soil organic matter, and the path toward a more quantitative
936 understanding. Global Change Biology 00:1–19
937 Wobbrock JO, Findlater L, Gergle D, Higgins JJ (2011) The aligned rank transformation for
938 nonparametric factorial analyses using only ANOVA procedures. In: Proceedings of the
939 ACM Conference on Human Factors in Computing Systems (CHI ’11). Vancouver,
940 British Columbia (May 7-12, 2011). ACM Press, New York, pp 143–146
941 Wolkovich EM, Lipson DA, Virginia RA, et al (2010) Grass invasion causes rapid increases
942 in ecosystem carbon and nitrogen storage in a semiarid shrubland. Global Change

943 Biology 16:1351–1365. doi: 10.1111/j.1365-2486.2009.02001.x
944 Xu C, Xu X, Ju C, et al (2021) Long-term, amplified responses of soil organic carbon to
945 nitrogen addition worldwide. Global Change Biology 27:1170–1180. doi:
946 10.1111/gcb.15489
947 Yahdjian L, Gherardi L, Sala OE (2011) Nitrogen limitation in arid-subhumid ecosystems: A
948 meta-analysis of fertilization studies. Journal of Arid Environments 75:675–680. doi:
949 10.1016/j.jaridenv.2011.03.003
950 Yang Y, Ji C, Ma W, et al (2012) Significant soil acidification across northern China's
951 grasslands during 1980s – 2000s. Global Change Biology 18:2292–2300. doi:
952 10.1111/j.1365-2486.2012.02694.x
953 Ye C, Chen D, Hall SJ, et al (2018) Reconciling multiple impacts of nitrogen enrichment on
954 soil carbon: plant, microbial and geochemical controls. Ecology Letters 21:1162–1173.
955 doi: 10.1111/ele.13083
956 Zak DR, Argiroff WA, Freedman ZB, et al (2019) Anthropogenic N deposition, fungal gene
957 expression, and an increasing soil carbon sink in the Northern Hemisphere. Ecology
958 100:e02804. doi: 10.1002/ecy.2804
959 Zeng D-H, Li L-J, Fahey TJ, et al (2010) Effects of nitrogen addition on vegetation and
960 ecosystem carbon in a semi-arid grassland. Biogeochemistry 98:185–193. doi:
961 10.1007/s10533-009-9385-x

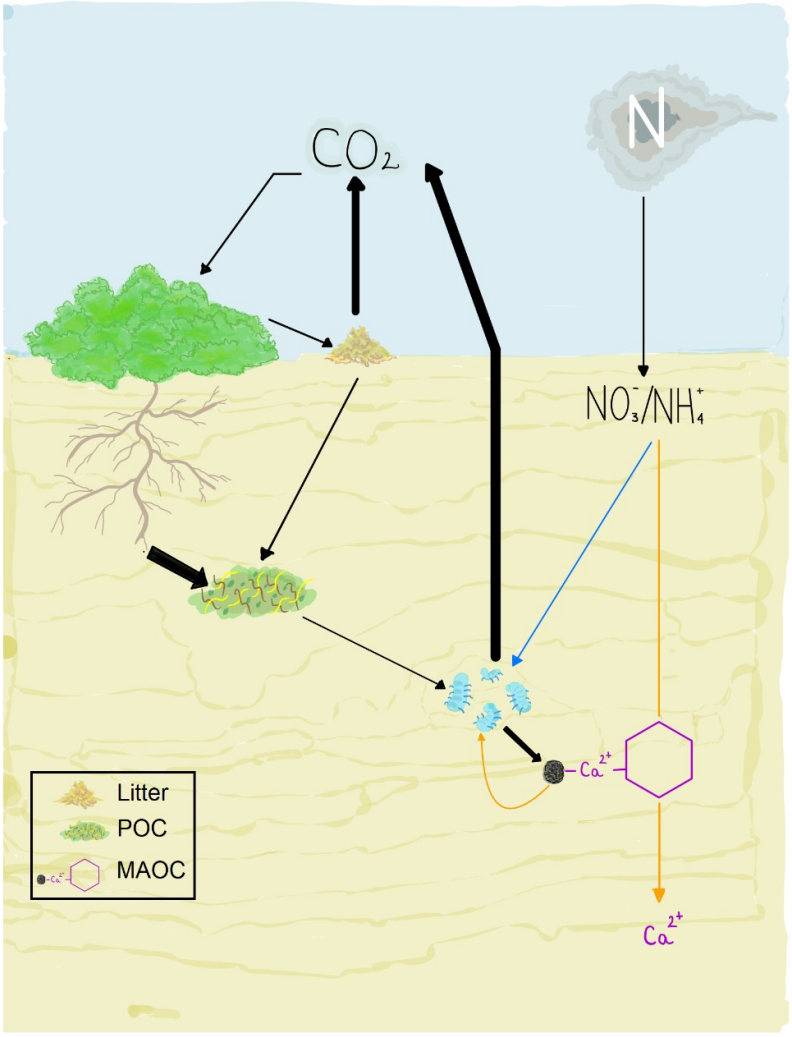

962

963 **Figure 1.** Conceptual overview of the processes that form soil organic C (SOC) as particulate
964 organic C (POC) and mineral-associated organic C (MAOC) at our site. Above- and
965 belowground litter is stored as POC in soils. A fraction of aboveground litter is photochemically
966 degraded aboveground and microbially decomposed to CO_2 before it can be stored as POC. POC
967 is relatively accessible to microbes in soils and can be decomposed via the microbial C pump to
968 form MAOC (Liang et al. 2017). A fraction of the POC decomposed by microbes is respired as
969 CO_2 during microbial metabolism. In dryland soils, calcium (Ca^{2+}) is important in bridging
970 negatively charged C compounds to negatively charged mineral surfaces to form MAOC.
971 Nitrogen enrichment can affect C storage by affecting microbial decomposition of POC and its
972 transformation into MAOC (blue arrow). Furthermore, nitrogen enrichment can acidify soils and

destabilize MAOC as Ca^{2+} is leached, making the C vulnerable to microbial decomposition (orange arrows). Arrow thickness represents the relative strength of the C flux between pools.

975 Figure 2

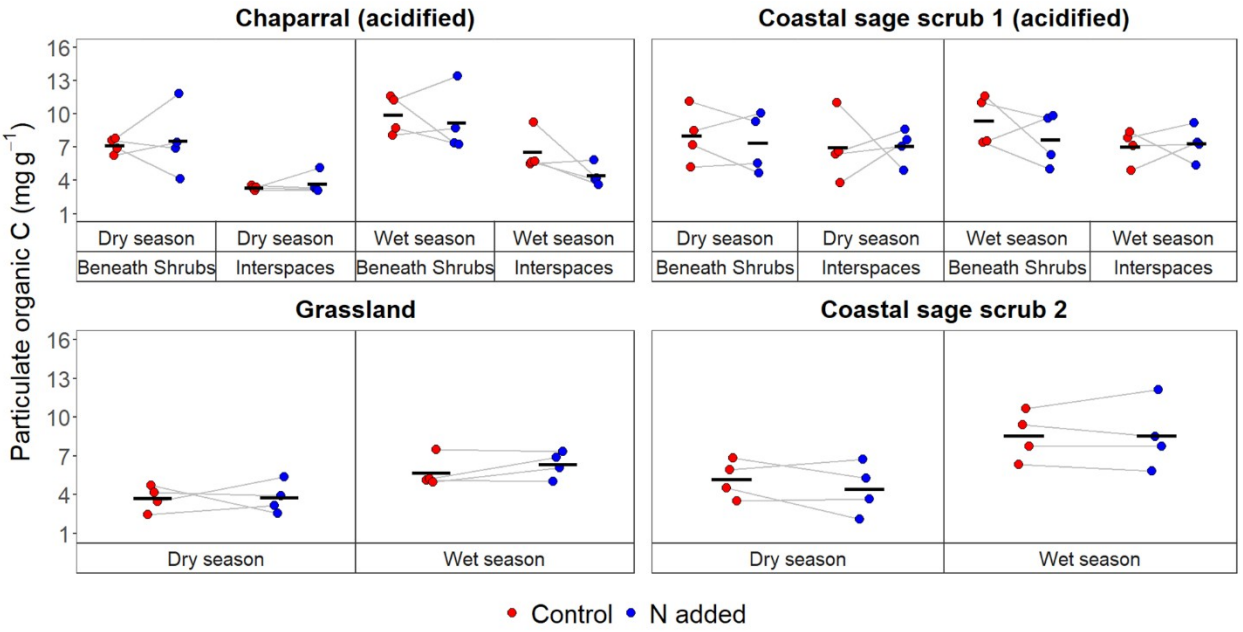

976

977 **Figure *2*.** Differences in particulate organic C (POC) between control and N-fertilized plots
978 during the dry season 2020 and the wet season 2021. At Chaparral and Coastal sage scrub 1,
979 soils were sampled beneath shrubs and in interspaces between shrubs. At Grassland and Coastal
980 sage scrub 2, soils were sampled beneath vegetation only. Chaparral and Coastal sage scrub 1
981 experienced strong acidification in response to N fertilization. Dots represent individual data
982 points (4 plots per treatment and soil position) with grey lines connecting paired control and N-
983 fertilized plots. Black crossbars represent means (n=4). If present, significant N fertilization
984 effects are indicated by black lines and asterisks directly above data points (*, $p<0.1$, **,
985 $p<0.05$).

Figure 3

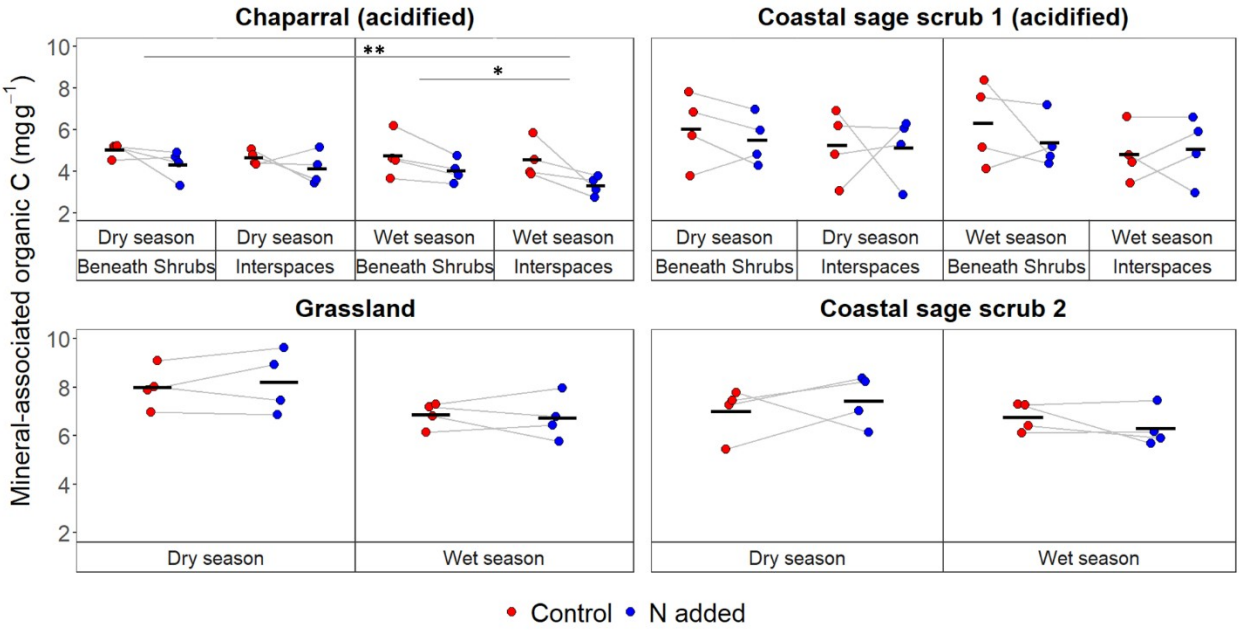

Figure *3.* Differences in mineral-associated organic C between control and N-fertilized plots during the dry season 2020 and the wet season 2021. At Chaparral and Coastal sage scrub 1, soils were sampled beneath shrubs and in interspaces between shrubs. At Grassland and Coastal sage scrub 2, soils were sampled beneath vegetation only. Chaparral and Coastal sage scrub 1 experienced strong acidification in response to N fertilization. Dots represent individual data points (4 plots per treatment and soil position) with grey lines connecting paired control and N-fertilized plots. Black crossbars represent means (n=4). If present, significant N fertilization effects are indicated by black lines and asterisks directly above data points (*, $p<0.1$, **, $p<0.05$)

Figure 4

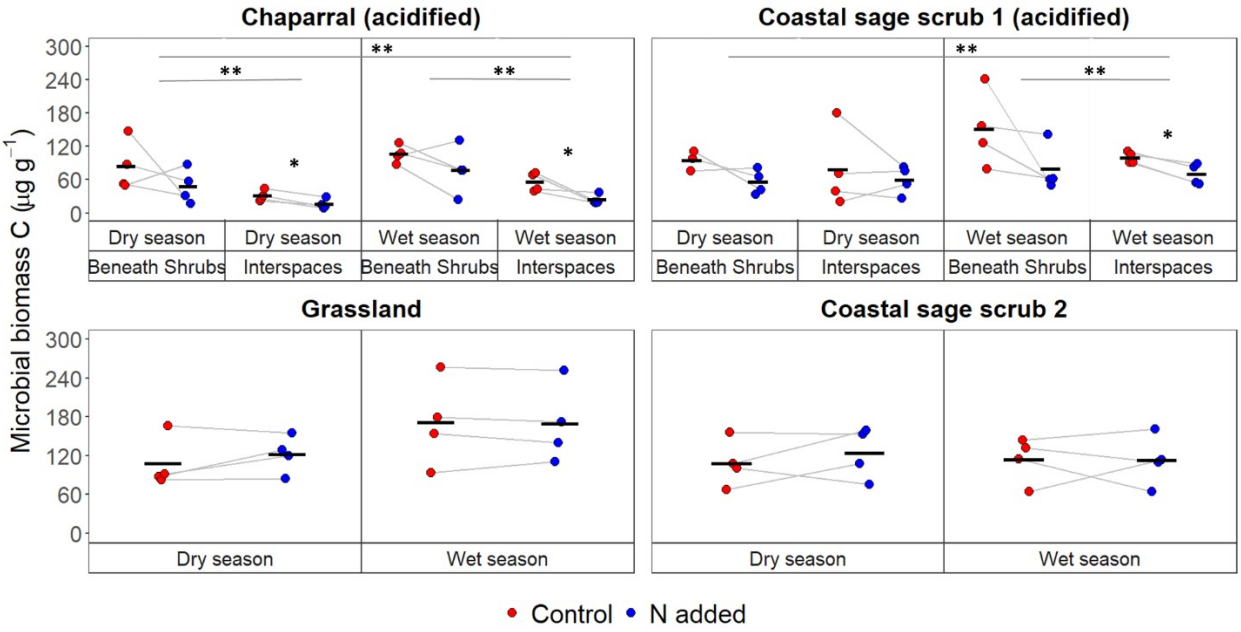

Figure 4. Differences in microbial biomass C between control and N-fertilized plots during the dry season 2020 and the wet season 2021. At Chaparral and Coastal sage scrub 1, soils were sampled beneath shrubs and in interspaces between shrubs. At Grassland and Coastal sage scrub 2, soils were sampled beneath vegetation only. Chaparral and Coastal sage scrub 1 experienced strong acidification in response to N fertilization. Dots represent individual data points (4 plots per treatment and soil position) with grey lines connecting paired control and N-fertilized plots. Black crossbars represent means (n=4). If present, significant N fertilization effects are indicated by black lines and asterisks directly above data points (*, $p<0.1$, **, $p<0.05$).

Figure 5

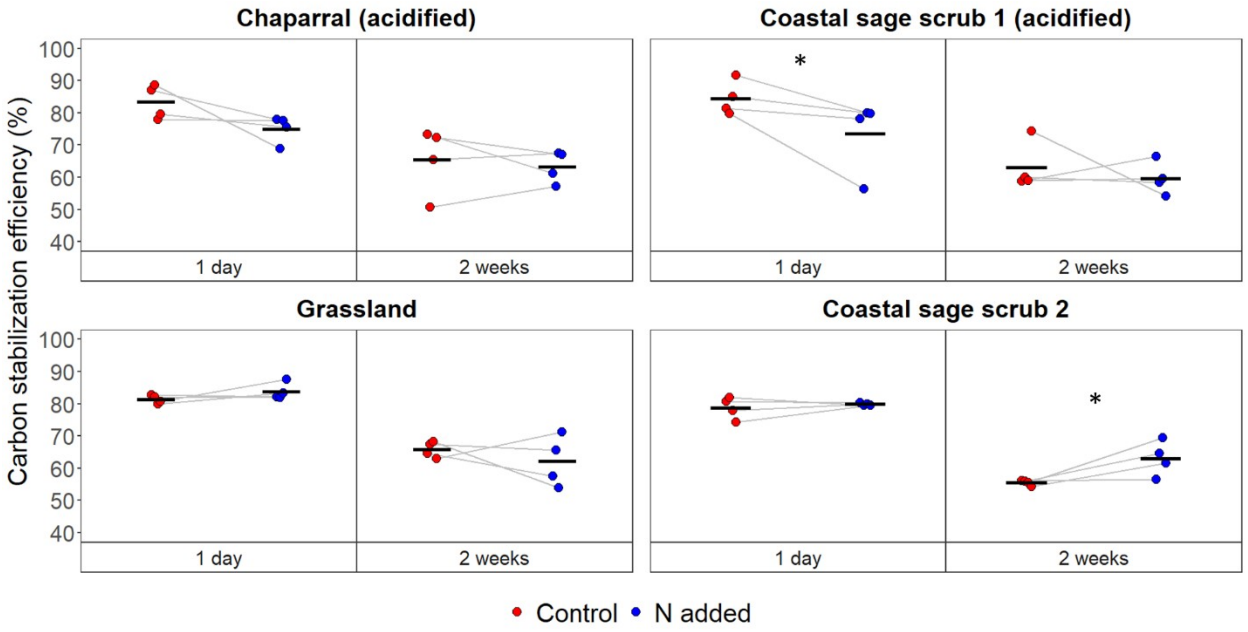

Figure 5. Differences in carbon stabilization efficiency measured in short- (1 day; i.e., community-scale carbon stabilization efficiency (CSE_c)) and long-term (2 weeks; i.e., ecosystem-scale carbon stabilization efficiency (CSE_E)) incubations between control and N-fertilized plots during the wet season 2021. Chaparral and Coastal sage scrub 1 experienced strong acidification in response to N fertilization. Dots represent individual data points (4 plots per treatment and soil position) with grey lines connecting paired control and N-fertilized plots. Black crossbars represent means (n=4). If present, significant N fertilization effects within each incubation time (paired t-test) are indicated by asterisks above data points (*, $p<0.1$, **, $p<0.05$).

Figure 6

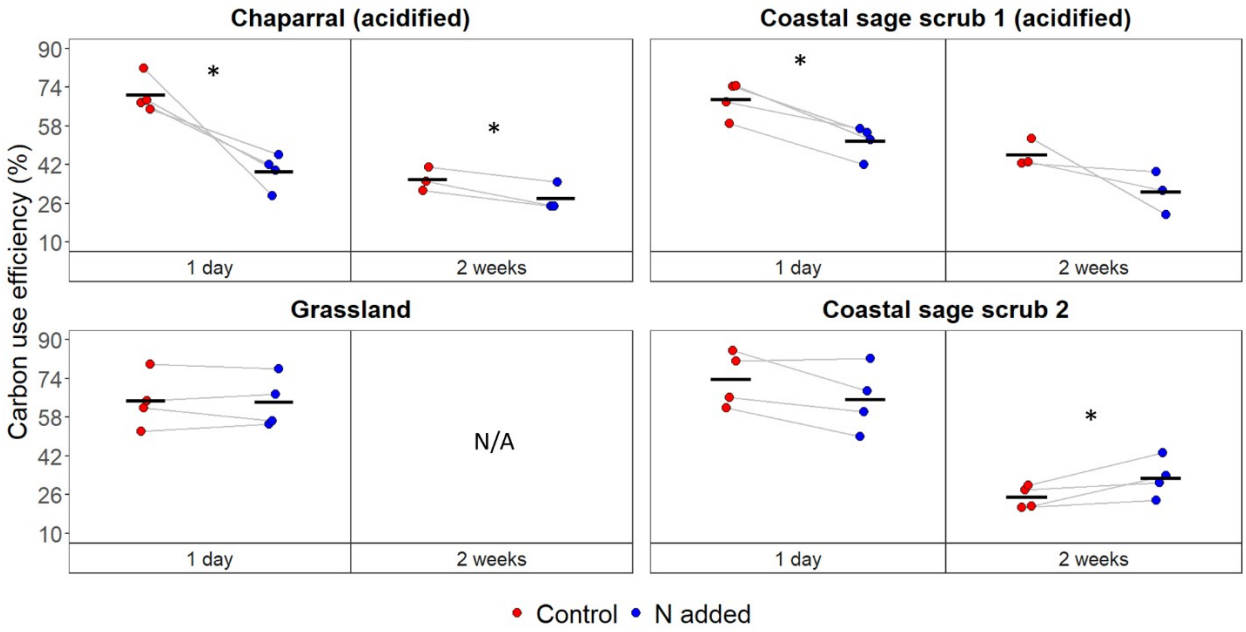

Figure 6. Differences in carbon use efficiency measured in short- (1 day; i.e., community-scale carbon use efficiency (CUE_c)) and long-term (2 weeks; i.e., ecosystem-scale carbon use efficiency (CUE_E)) incubations between control plots and plots fertilized with N during the wet season 2021. Chaparral and Coastal sage scrub 1 experienced strong acidification in response to N fertilization. Dots represent individual data points (4 plots per treatment and soil position) with grey lines connecting paired control and N-fertilized plots. Black crossbars represent means (n=4). For the 2-week incubation, one sample was lost for Chaparral and Coastal sage scrub 1 (n=3) and Grassland has no data because CUE could not be calculated (see methods). If present, significant N fertilization effects within each incubation time (paired t-test) are indicated by asterisks above data points (*, $p<0.1$, **, $p<0.05$).

Figure 7

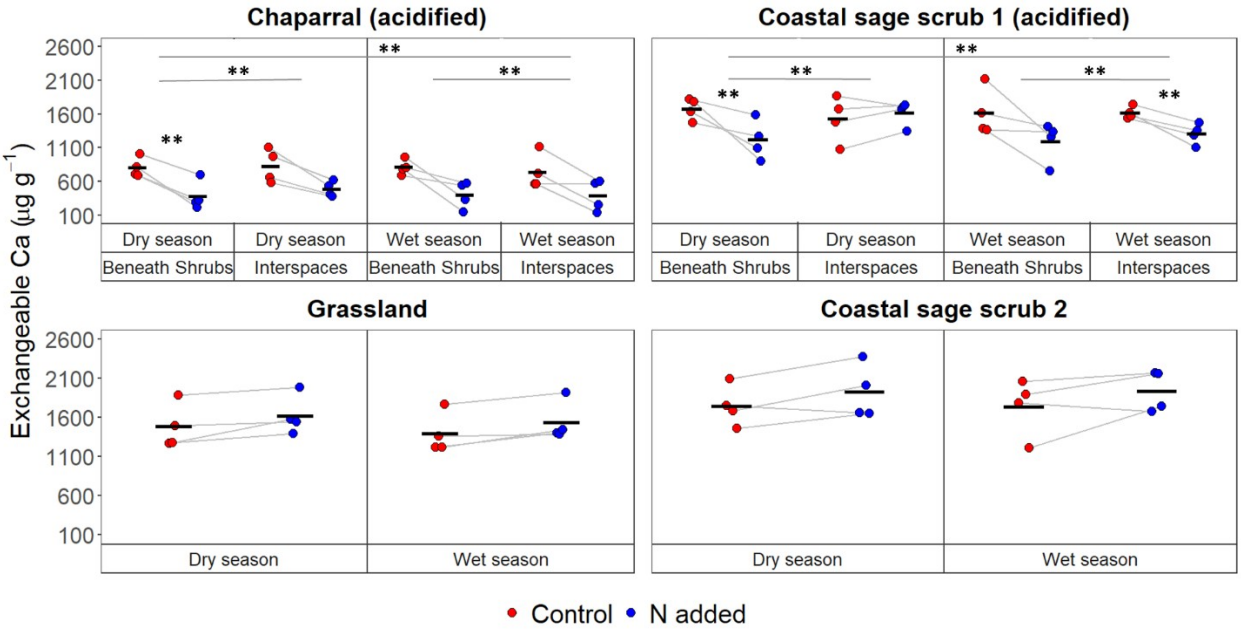

Figure 7. Differences in soil exchangeable Ca between control and N-fertilized plots during the dry season 2020 and the wet season 2021. At Chaparral and Coastal sage scrub 1, soils were sampled beneath shrubs and in interspaces between shrubs. At Grassland and Coastal sage scrub 2, soils were sampled beneath vegetation only. Chaparral and Coastal sage scrub 1 experienced strong acidification in response to N fertilization. Dots represent individual data points (4 plots per treatment and soil position) with grey lines connecting paired control and N-fertilized plots. Black crossbars represent means (n=4). If present, significant N fertilization effects are indicated by black lines and asterisks directly above data points (*, $p<0.1$, **, $p<0.05$).

Figure 8

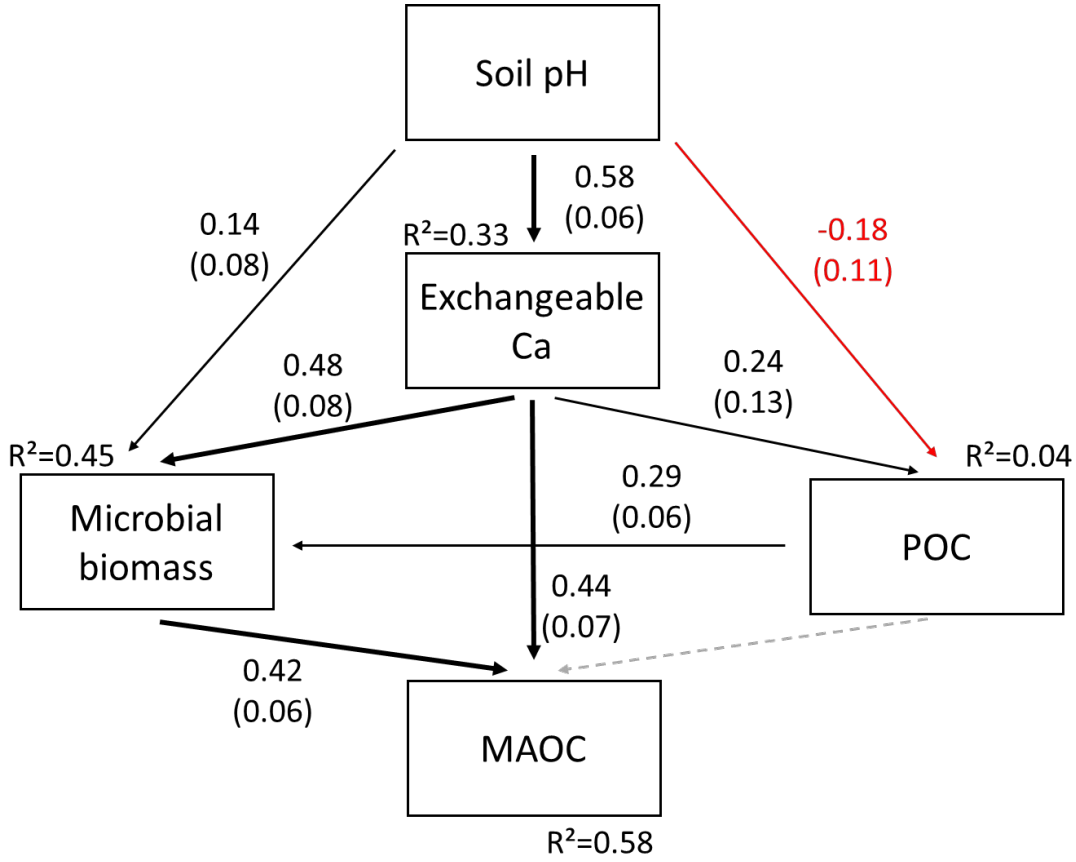

Figure 8. Structural equation model depicting how measured soil variables (n = 96) affect particulate organic C (POC) and mineral-associated organic C (MAOC) across control and N-fertilized plots during the dry season 2020 and the wet season 2021. Numbers next to boxes indicate the variation in the variable explained by the pathways leading to it. Numbers next to arrows indicate standardized path coefficients (robust standard errors of coefficients). Red lines indicate negative relationships and grey, dashed lines indicate non-significant pathways ($p > 0.1$). Thickness of arrows represent the relative importance of pathways. Model statistics: Robust χ^2 = 2.279 ($p = 0.131$), robust comparative fit index (CFI) = 0.993, robust root mean square error of approximation (RMSEA) = 0.115.

Table 1. Site description. MAP is mean annual precipitation.

	MAP (mm)	Dominant vegetation cover type	Fire history	Soil texture class	Background N deposition (kg N ha^{-1} y^{-1})	N fertilization rate (kg N ha^{-1} y^{-1})	Form of N added	Duration of N fertilization
CHAP	382	Evergreen shrubland	Burned 2003	Loamy sand	2-4	50	NH_4NO_3 (2003–2007) (NH4)2SO4 (2007–2009) urea (2009-present)	17-18 years
CSS1	414	Drought-deciduous shrubland	No data	Sandy loam	2-4	50	NH_4NO_3 (2003–2007) (NH4)2SO4 (2007–2009) urea (2009-present)	17-18 years
GRASS	281	Annual grassland	Burned 2007 and 2020	Sandy loam	15	60	$CaNO_3$	13-14 years
CSS2	281	Drought-deciduous shrubland	Burned 2007 and 2020	Sandy loam	15	60	$CaNO_3$	13-14 years

Table 2. Soil characteristics. Values are means (standard deviation; n=4). Numbers in bold indicate significant differences between control and N-fertilized plots evaluated in a three-way ANOVA across seasons and ~~soil positions~~microhabitats for CHAP and CSS1, but in a two-way ANOVA across seasons for GRASS and CSS2 ($p<0.1$). For NH_4^+ and NO_3^-, ANOVAs were performed on aligned rank transformed data to account for non-normality and unequal variances. WEOC is water-extractable organic C.

		Soil pH		Sand fraction C (mg g^{-1})		Soil organic C (mg g^{-1})		Soil organic N (mg g^{-1})		Soil organic C:N		WEOC (µg g^{-1})		NH_4^+ (µg g^{-1})		NO_3^- (µg g^{-1})	
		Control	N added	Control	N added	Control	N added	Control	N added	Control	N added	Control	N added	Control	N added	Control	N added
		Dry Season (Oct 2020)															
CHAP	Shrub	6.52 (0.18)	**4.89 (0.37)**	1.98 (0.32)	1.88 (0.42)	13.58 (1.66)	**12.49 (3.36)**	0.57 (0.1)	0.56 (0.14)	28.36 (3.45)	**25.95 (1.21)**	88.39 (10.80)	70.60 (8.46)	0.57 (0.22)	**11.98 (18.14)**	0.08 (0.06)	**1.00 (0.74)**
	Inter-space	6.51 (0.16)	**5.22 (0.29)**	1.84 (0.52)	1.56 (0.28)	9.63 (1.07)	**8.68 (1.09)**	0.39 (0.04)	0.42 (0.08)	28.73 (3.76)	**24.67 (2.36)**	61.17 (7.43)	51.83 (14.73)	0.60 (0.09)	**2.78 (1.89)**	0.21 (0.12)	**1.52 (1.00)**
CSS1	Shrub	6.52 (0.12)	**5.36 (0.22)**	0.57 (0.19)	0.80 (0.13)	12.92 (3.21)	13.38 (1.89)	0.85 (0.20)	0.92 (0.12)	17.66 (0.66)	**16.98 (0.53)**	165.46 (41.85)	176.09 (34.35)	1.44 (0.28)	**6.81 (3.43)**	0.87 (0.35)	**1.33 (0.68)**
	Inter-space	6.58 (0.13)	**5.91 (0.56)**	0.69 (0.37)	0.93 (0.41)	12.54 (6.94)	13.23 (4.71)	0.82 (0.44)	0.91 (0.30)	17.48 (0.86)	**16.73 (0.75)**	154.44 (43.87)	160.32 (18.73)	2.21 (1.65)	**4.08 (1.83)**	1.18 (0.26)	**3.13 (3.47)**
GRASS		6.44 (0.09)	6.39 (0.17)	0.98 (0.29)	1.13 (0.46)	14.34 (1.99)	14.11 (2.15)	1.33 (0.17)	1.32 (0.15)	12.61 (0.42)	12.45 (0.75)	131.33 (22.61)	129.30 (22.86)	2.55 (2.62)	4.84 (3.98)	8.16 (4.21)	**26.07 (7.25)**
CSS2		6.31 (0.13)	6.59 (0.10)	0.53 (0.11)	0.61 (0.16)	13.57 (2.03)	14.29 (1.20)	1.09 (0.15)	1.15 (0.12)	14.46 (0.38)	14.58 (0.80)	133.08 (18.72)	161.79 (27.80)	0.79 (0.26)	0.95 (0.31)	0.79 (0.31)	**1.62 (0.24)**

		Wet Season (April 2021)													
CHAP	Shrub	6.64 (0.35)	**4.90 (0.11)**	1.98 (0.26)	1.77 (0.23)	15.90 (4.07)	**13.44 (3.59)**	0.65 (0.20)	**0.63 (0.19)**	29.44 (4.19)	**24.97 (1.78)**	37.94 (7.24)	51.08 (25.62)	0.40 (0.21)	**6.90 (4.22)**	0.06 (0.10)	**12.72 (5.84)**
	Inter-space	6.63 (0.26)	**5.07 (0.25)**	1.98 (0.31)	1.91 (0.41)	13.03 (3.91)	**8.68 (0.56)**	0.61 (0.29)	**0.39 (0.09)**	27.68 (5.58)	**27.37 (5.28)**	20.25 (8.58)	17.84 (5.80)	0.45 (0.29)	**9.04 (8.44)**	0.06 (0.08)	**7.27 (4.61)**
CSS1	Shrub	6.53 (0.19)	**5.20 (0.46)**	0.74 (0.34)	0.54 (0.09)	16.17 (4.88)	11.89 (3.08)	1.16 (0.35)	0.97 (0.31)	16.30 (1.19)	**14.51 (1.17)**	85.47 (23.95)	124.73 (62.75)	0.81 (0.27)	**6.92 (4.50)**	0.76 (0.55)	**19.43 (10.80)**
	Inter-space	6.82 (0.25)	**5.17 (0.13)**	0.50 (0.07)	0.58 (0.21)	11.73 (4.78)	12.50 (3.39)	0.82 (0.32)	0.99 (0.32)	16.51 (0.58)	**15.01 (1.63)**	83.10 (21.17)	91.70 (30.06)	1.70 (1.08)	**3.19 (2.18)**	3.83 (4.80)	**42.42 (10.97)**
GRASS		6.31 (0.23)	6.58 (0.17)	0.80 (0.17)	0.95 (0.17)	13.65 (1.02)	13.69 (2.37)	1.22 (0.11)	1.25 (0.23)	13.11 (0.45)	12.79 (0.32)	81.63 (4.71)	137.57 (95.55)	0.97 (0.22)	1.50 (0.25)	0.60 (0.23)	**3.43 (1.00)**
CSS2		6.55 (0.36)	6.61 (0.20)	0.68 (0.07)	0.57 (0.06)	14.78 (2.20)	15.37 (3.22)	1.22 (0.15)	1.29 (0.26)	14.11 (0.71)	13.89 (0.47)	83.79 (22.43)	74.20 (12.55)	1.79 (0.70)	2.37 (0.70)	3.81 (2.21)	**14.26 (5.14)**

1059

Table 2. Soil extracellular enzymes measured and their abbreviations and functions.

Enzyme	Abbreviation	Function
α-glucosidase	AG	Starch degradation; C acquisition
1,4-β-cellobiohydrolase	CBH	Cellulose degradation; C acquisition
β-glucosidase	BG	Cellulose degradation; C acquisition
N-acetyl-ß-D-glucosaminidase	NAG	Chitin degradation; N acquisition
L-Leucine aminopeptidase	LAP	Peptide breakdown; N acquisition
Phosphomonoesterase	PHO	Organic phosphorus degradation; P acquisition

Table 3. Potential activities of C-acquiring soil extracellular enzymes alpha-glucosidase (AG), beta-glucosidase (BG) and cellobiohydrolase (CBH), N-acquiring soil extracellular enzymes N-acetyl-glucosaminidase (NAG) and leucine-aminopeptidase (LAP) and P-acquiring soil extracellular enzyme phosphomonoesterase (PHO). Data are means (standard deviation). Numbers in bold indicate significant differences between control and N-fertilized plots with N evaluated in a Three-way mixed ANOVA across seasons and ~~soil positions~~microhabitats for CHAP and CSS1 and in a Two-way ANOVA across seasons for GRASS and CSS2 ($p<0.1$).

		AG (nmol g^{-1} h^{-1})		CBH (nmol g^{-1} h^{-1})		BG (nmol g^{-1} h^{-1})		NAG (nmol g^{-1} h^{-1})		LAP (nmol g^{-1} h^{-1})		PHO (nmol g^{-1} h^{-1})	
		Control	N added	Control	N added	Control	N added	Control	N added	Control	N added	Control	N added
		Dry Season (October 2020)											
CHAP	Shrub	8.3 (0.6)	**3.0 (0.9)**	14.6 (5.0)	**9.9 (8.6)**	315.9 (79.5)	**135.1 (98.7)**	60.4 (14.7)	**39.5 (24.9)**	64.0 (7.1)	**27.4 (8.5)**	195.5 (29.5)	**72.8 (27.0)**
	Interspace	3.4 (0.8)	**1.9 (0.8)**	4.0 (2.3)	**2.0 (0.9)**	94.7 (39.0)	**39.6 (19.0)**	25.0 (6.7)	**12.5 (5.4)**	50.2 (29.0)	**19.8 (5.7)**	130.1 (51.1)	**64.1 (28.0)**
CSS1	Shrub	9.0 (0.9)	**4.6 (1.1)**	22.6 (8.5)	**10.6 (3.1)**	341.4 (109.2)	**119.0 (29.1)**	103.8 (30.6)	74.1 (14.4)	90.2 (13.7)	**46.4 (6.4)**	366.6 (59.8)	**173.7 (44.4)**
	Interspace	9.8 (3.8)	**6.0 (1.3)**	15.4 (8.8)	**11.6 (3.8)**	218.7 (124.4)	**154.5 (35.1)**	94.2 (59.2)	82.1 (19.9)	89.8 (35.5)	**61.6 (16.6)**	349.6 (132.0)	**221.0 (66.3)**
GRASS		13.7 (1.6)	13.7 (1.6)	42.2 (19.9)	54.0 (11.1)	405.3 (123.1)	436.1 (107.0)	139.6 (45.2)	161.6 (28.4)	131.3 (31.6)	136.0 (32.0)	580.5 (141.8)	622.7 (107.3)
CSS2		9.2 (1.8)	9.5 (3.1)	23.8 (12.4)	30.5 (22.6)	232.8 (91.6)	268.2 (139.7)	72.3 (21.4)	93.1 (32.5)	78.6 (16.5)	92.7 (27.4)	414.4 (82.3)	476.9 (201.4)
		Wet Season (April 2021)											
CHAP	Shrub	7.8 (1.6)	**4.0 (1.3)**	17.3 (8.7)	**6.7 (2.3)**	259.5 (118.9)	**98.7 (24.6)**	64.0 (26.9)	**27.0 (9.4)**	73.4 (20.5)	**25.5 (3.8)**	174.8 (80.7)	**80.3 (25.6)**
	Interspace	4.7 (1.3)	**3.0 (1.3)**	4.7 (1.3)	**3.0 (1.1)**	81.1 (32.2)	**25.4 (15.4)**	29.7 (17.8)	**9.2 (2.6)**	41.2 (9.7)	**13.8 (2.4)**	116.7 (47.4)	**49.3 (17.1)**
CSS1	Shrub	9.0 (1.2)	**4.3 (1.6)**	24.2 (7.0)	**9.7 (3.8)**	332 (162.7)	**108.5 (30.3)**	80.2 (18.4)	64.5 (8.9)	121.7 (23.2)	**50.0 (21.0)**	384.2 (106.2)	**222.2 (59.5)**
	Interspace	6.5 (2.1)	**3.4 (1.1)**	9.8 (3.6)	**5.3 (1.2)**	123.2 (26.7)	**75.2 (14.0)**	46.9 (11.4)	70.0 (13.2)	73.4 (13.0)	**48.9 (6.6)**	237.4 (48.6)	**189.6 (43.6)**

GRASS	10.2 (1.4)	9.1 (1.8)	33.4 (8.5)	36.3 (12.6)	306.6 (35.8)	282.8 (73.4)	94.6 (6.3)	98.7 (16.7)	128.5 (5.8)	133.8 (24.1)	482.0 (78.1)	483.5 (143.8)
CSS2	8.4 (2.6)	7.0 (0.8)	20.3 (7.5)	18.2 (6.2)	204.0 (53.9)	162.3 (49.4)	57.9 (20.4)	62.7 (11.1)	99.8 (23.9)	102.7 (14.1)	391.0 (67.0)	394.6 (59.8)

1068